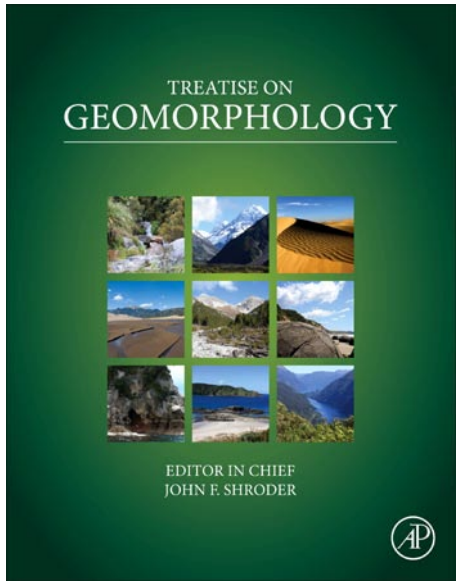

Marticorena B., and Formenti P. (2013) Fundamentals of Aeolian Sediment Transport: Long-Range Transport of Dust. In: John F. Shroder (ed.) Treatise on Geomorphology, Volume 11, pp. 64-84. San Diego: Academic Press.

11.5 Fundamentals of Aeolian Sediment Transport: Long-Range Transport of Dust

B Marticorena and P Formenti, Laboratoire Interuniversitaire des Systèmes Atmosphériques, Créteil, France

Glossary

Aerosol optical thickness (AOT) Extinction by atmospheric aerosols of the solar radiation along a vertical atmospheric column.

Angström coefficient Spectral dependence of the AOT that depends on aerosol size.

Aspect ratio (AR) Ratio of the longest dimension to the orthogonal width of particles.

Direct radiative effect efficiency Flux perturbation in a given spectral domain (visible or infrared) normalized by the aerosol optical depth (DRE/AOD, units of $W\,m^{-2}$).

Single scattering albedo Ratio of scattering to total light extinction (absorption plus scattering).

Abstract

Mineral dust has the capability to be transported from its source regions as far as thousands of kilometers away. The first quantitative evidence of long-range transport of mineral dust was provided by *in situ* surface monitoring of aerosol composition in the early 1970s. Since the 1980s the investigation of this long-range transport has strongly benefited from the development of satellite imagery. The temporal resolution of satellite imagery also allows tracking of individual dust storms from their source regions and along their transport paths. It also provides quantitative information on the aerosol atmospheric content and thus an estimation of the intensity of mineral dust export. Extensive information on the mineral dust spatial distribution and physico-chemical properties has been provided by large and extensive field campaigns. From all these information sources, global pictures of the main transport pattern in the regions where this transport is the most intense have been established; some mechanisms responsible for its variability at the seasonal and interannual scale have been described and the amount of dust transported has been quantified.

The objective of this chapter is to give an overview on the global distribution and the magnitude of dust long-range transport in the atmosphere, and on its temporal variability in regions where mineral dust transport it is the most intense, that is, the North Atlantic and North Pacific Ocean. The ways in which dust physical and chemical properties can be affected by long-range transport and the consequences in terms of mineral dust impact are discussed.

Marticorena, B., Formenti, P., 2013. Fundamentals of aeolian sediment transport: long range transport of dust. In: Shroder, J. (Editor in Chief), Lancaster, N., Sherman, D.J., Baas, A.C.W. (Eds.), Treatise on Geomorphology. Academic Press, San Diego, CA, vol. 11, Aeolian Geomorphology, pp. 64–84.

11.5.1 Introduction

Aeolian erosion in arid and semiarid regions is the main source of atmospheric dust particles. Although mineral dust is composed of relatively large particles (mass-median diameter $\sim$1.5–3 μm) compared to other tropospheric aerosols, it has the capability to be transported from its source regions as far as thousands of kilometers away. For instance, mineral dust raised over the central Asian deserts has been observed over the North Pacific Ocean as far as 5000 km from the source region (i.e., Husar et al., 2001), and Saharan dust is regularly observed on the western side of the tropical Atlantic (i.e., Prospero, 1968). This transport taking place over thousands of km is commonly referred to as long-range transport.

Charles Darwin, one of the first reporting on long-range transport of mineral dust, attributed an African origin to the mineral dust deposited on ships in the Atlantic Ocean (Darwin, 1846). Although mentions of 'red rains' over Europe, 'yellow sand' or 'Kosa' events over Korea or Japan can be found in historical records, scientific studies on this phenomenon started only at the end of the 1960s and early 1970s, and further developed since the end of the 1970s due to an increasing capability to observe and quantify this long-range transport.

In situ surface monitoring of aerosol composition provides the first nonambiguous and quantitative evidence of mineral dust long-range transport. Such a monitoring was initiated in 1966 at Barbados (Prospero, 1968). Barbados was selected in the framework of a program dedicated to the measurements of of extraterrestrial dust in the atmosphere, as a site providing a clean air environment (Delany et al., 1967). The mineralogical and biological composition of the sampled red dust finally allowed pointing out its African origin. This has been a starting point for the establishment the longest and most famous dust concentration time series of mineral dust concentration in deposition regions. This time series has been used to evaluate the intensity of the long-range transport of Saharan dust (Prospero, 1968) and the investigation of its seasonal (Prospero and Carlson, 1981) and interannual variability (Prospero and Nees, 1986). A similar approach has been adopted in other location of the world to investigate mineral dust transport at several transport or deposition regions located downwind of the main dust sources, that is, the Mediterranean basin (i.e., Bergametti et al., 1989; Kubilay et al., 2000), the north Atlantic African coast (i.e., Jaenicke and Schütz, 1978, Chiapello et al., 1997) and downwind Asia (i.e., Uematsu et al., 1986; Duce et al., 1980). Scientific cruises, mainly motivated by the evaluation of the contribution of atmospheric deposition to nutrient input to the ocean, also provided measurements of mineral dust concentrations in remote oceanic areas (i.e., concentrations reported by Duce, 1995).

The investigation of long-range transport of mineral dust has strongly benefited from the development of satellite imagery in the 1980s. Impressive images of dust plumes coming out from north Africa and Asia provide a dramatic portrayal of the intensity and extent of long-range transported dust. The temporal resolution of satellite imagery also allows tracking of individual dust storms from their source regions and all along their transport paths, that is, from the west coast of Africa to the east coast of USA for Saharan dust (Ott et al., 1991) or from Asian Eastern coats to the West coast of USA (Takayama and Takashima, 1986; Husar et al., 2001). Over the ocean, satellite retrieval provides quantitative information on the aerosol atmospheric content and thus an estimation of the intensity of mineral dust export. Husar et al. (1997), using National Oceanic and Atmospheric Administration/Advanced Very High Resolution Radiometer (NOAA/AVHRR) satellite images, showed that marine regions where the largest aerosol optical depths are observed are located downwind of the main deserts of the Earth.

In the late 1980s and beginning of the 1990s, the impact of tropospheric aerosols on the Earth's radiative budget, and thus on climate, motivated setting up large and extensive field campaigns dedicated to the description of aerosol spatial distribution and physico-chemical properties. These experiments provide a unique opportunity to investigate regional patterns and meteorological processes associated with mineral dust transport, but their main purpose is to provide a complete documentation of the aerosol's properties, including the size distribution and composition. Most of these field campaigns have been conducted in transport regions such as the 2nd Aerosol Characterization Experiment (ACE-2) over the Canary Islands (Raes et al., 2000), the Puerto Rico Dust Experiment (PRIDE) (Reid et al., 2003a), the Saharan Dust Experiment (SHADE) (Haywood et al., 2003; Tanre et al., 2003) over the Cape Verde Islands, and ACE-Asia field experiment (Huebert et al., 2003). More recently, field experiments have been conducted within source regions or in their vicinity: in China (Aeolian Dust Experiment on Climate impacts (ADEC); Mikami et al., 2002), in the Arabian Gulf (United Arab Emirates Unified Aerosol Experiment (UAE2); Reid et al., 2008), in Sahelian West Africa (African Monsoon Multidisciplinary Analysis (AMMA); Haywood et al., 2008), and in North Africa (Saharan Mineral Dust Experiment (SAMUM-1) Heintzenberg, 2008).

Long-term time series of near surface dust concentrations and satellite imagery have been used to investigate the annual to decadal variability of long-range dust transport. Prospero and Nees (1986) showed that between 1964 and 1984, mineral dust concentrations over the north tropical Atlantic Ocean increased simultaneously with the decrease of precipitation over the Sahel in Africa. Based on the analysis of data from different satellite sensors, Chiapello et al. (2005) showed how the mineral dust content over the Atlantic Ocean can be connected not only to the precipitation in the Sahel but also to large-scale meteorology via the North Atlantic Oscillation index. From a statistical trend analysis of this time series, Moulin and Chiapello (2006) suggested that part of the increase in the dust content over the north tropical Atlantic Ocean in the past 20 years can be attributed to land-use in the semiarid areas of the Sahel. More recently, additional information on the aerosol distribution from ground-based or spaceborne lidar systems (i.e., Liu et al., 2008) further reinforce the analysis of the meteorological situations responsible for mineral dust transport by providing a quantitative description of mineral dust vertical distribution in the atmosphere, from the sources toward the transport regions.

From all this information, global pictures of the mechanisms responsible for the main transport pattern in the regions where this transport is the most intense have been established, its variability at the seasonal and interannual scale have been described, and the amount of dust concerned by this transport has been quantified.

In this chapter, we first describe the global distribution and order of magnitude of the intensity of dust long-range transport in the atmosphere. In a second part, the temporal variability of the long-range transport in regions where it is the most intense, that is, the North Atlantic and North Pacific Ocean, is discussed regarding the meteorological conditions responsible for this transport. The third part concerns the way dust physical and chemical properties can be affected by long-range transport. Finally, we briefly discuss the main impacts motivating the investigation and quantification of mineral dust long-range transport.

11.5.2 Dust Transport Patterns and Pathways

The regions affected by long-range transport of mineral dust are can be located many thousands of kilometers downwind of source regions. Thus, the spatial distribution and the amount of dust transported depend not only on the intensity of dust emissions in the source regions but also on the meteorological processes responsible for transport away from sources.

11.5.2.1 Spatial Patterns

The spatial distribution of transported mineral dust was initially investigated by collecting and summarizing available surface measurements of atmospheric dust concentrations. Chester (1986) reported on the range of dust concentrations over oceans, and Duce (1995) reported some typical concentrations over continents. From these two data sets (**Figure 1**), mean mineral dust concentrations measured all over the world span more than 6 orders of magnitude. The measured dust concentrations are the highest downwind of the Sahara Desert and the Arabian Peninsula. Typical concentrations range more than 3 orders of magnitude, with maximum concentrations on the order of 1000 $\mu g\ m^{-3}$. Concentrations reported over the North Pacific Ocean, downwind of Asian deserts, are lower (minimum values lower than 1 $\mu g\ m^{-3}$, but ranging up to values on the order of 100 $\mu g\ m^{-3}$). Concentrations downwind of Australia are of the same order of magnitude as over the North Pacific Ocean. Extremely low but detectable dust concentrations are measured within or close to polar regions, with typical concentrations ranging from 00.1 to 0.001 $\mu g\ m^{-3}$ in the Southern Hemisphere, and concentrations on the order of magnitude higher in the Northern Hemisphere areal. This difference can be explained by the fact that mineral dust emissions are much higher in the Northern Hemisphere where arid and semiarid areas cover much larger surfaces than in the Southern Hemisphere. This average

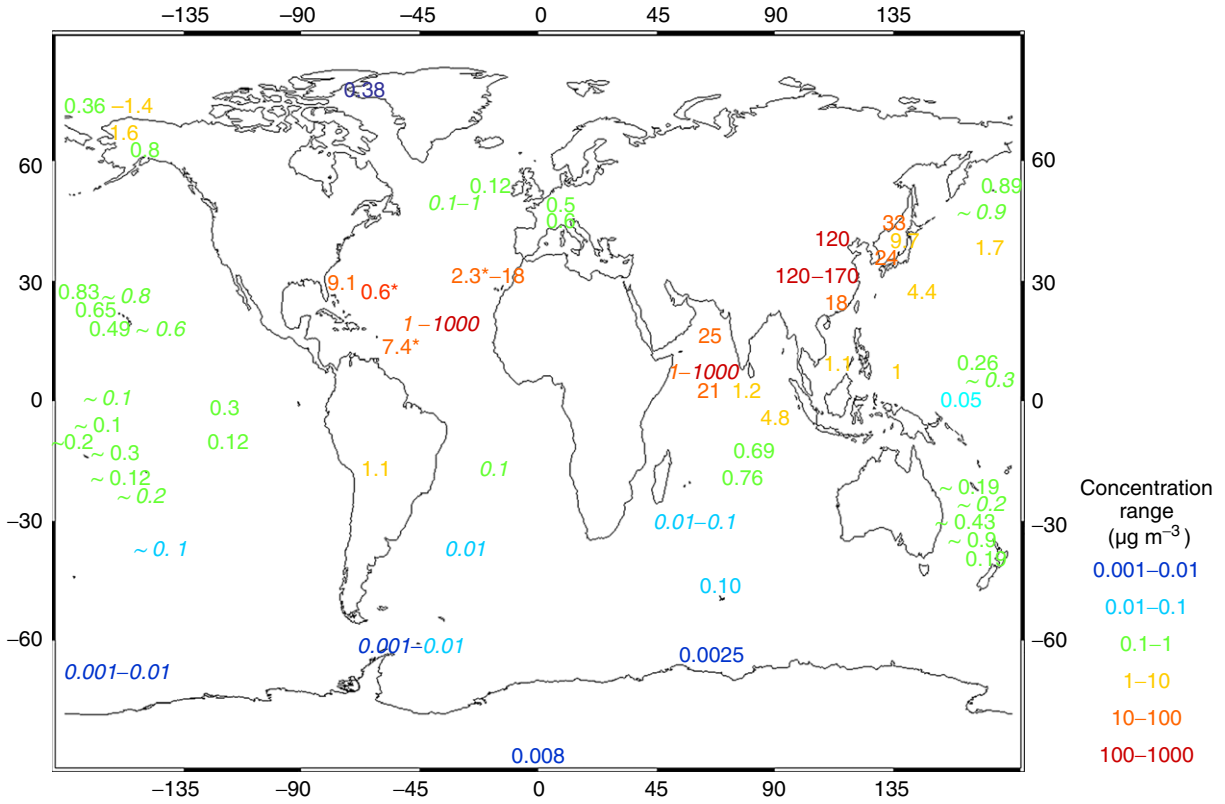

Figure 1 Typical mineral dust concentrations ($\mu g\ m^{-3}$) measured over oceanic and continental areas. Data from Chester, R.,1986. The marine mineral aerosol. In: Buat-Ménard, P. (Ed.), The Role of Air–Sea Exchange in Geochemical Cycling. D. Reidel Publishing Company, Dordrecht, pp. 443–476 (in italics) and Duce, R.A.,1995. Sources, distributions, and fluxes of mineral aerosols and their relationship to climate. In: Charlson, R.J., Heintzenberg, J. (Eds.), Aerosol Forcing of Climate. Wiley, New York, pp. 43–72.

picture is obviously biased by the scarcity and heterogeneous distribution of the available measurements and also by the fact that the reported concentrations are averages. At the scale of individual dust events, the surface concentrations can reach much higher values. As an example, Tsunogai and Kondo (1982) described how the occurrence of a dust transport event raised surface concentration of Al measured onboard a ship in the North Pacific Ocean from 30–50 up to 670 n gm^{-3} (i.e., ~375–8400 μg m^{-3} of mineral dust assuming the mean Al content in the Earth's crust is on the order of 8% (Taylor and McLennan, 1985)).

Most of these data are derived from chemical analysis of elements considered as proxies of mineral dust (generally Al or Fe), using, as mentioned above, the mean mass ratios that these elements would have in the Earth's crust (typically ~8% for Al and 5% for Fe (Taylor and McLennan, 1985)). This approach allows identification of the mineral dust component in the atmospheric aerosol load. The main restriction for this type of estimates comes from the fact that such measurements are usually performed at the surface level, in ground-based stations or onboard ship, and thus document surface concentrations only. Such measurements are also possible on airborne platforms and are now commonly deployed during intensive field campaigns. However, aircraft sampling remains challenging, due to the difficulties in reproducing, without biases, the particle size distribution at high air speeds such as those experienced during flights (Wendisch et al., 2004). In addition, aircraft campaigns are necessarily limited in duration, so their temporal representativeness is limited, whereas surface concentrations can be monitored only locally, but over longer time periods.

The global picture of mineral dust transport has been significantly improved by global aerosol products from satellite imagery. Dust aerosols have the capability to scatter and absorb solar radiation in the visible spectrum and can thus be simply portrayed in visible satellite imagery. Examples of dust plumes imaged at visible wavelengths are shown in **Figure 2**.

Quantitative measurements of the atmospheric aerosol load can be derived from satellite measurements of backscattered radiation. The columnar extinction of solar radiation by atmospheric aerosols is quantified by the Aerosol Optical Thickness (AOT). For a given aerosol type, and assuming homogeneous properties along the atmospheric column, the AOT is proportional to the vertically integrated atmospheric concentration weighted by the extinction efficiency. The extinction efficiency is itself largely controlled by the aerosol size-distribution and composition. The spectral dependence of the AOT, the Angstrom coefficient, can be used to discriminate aerosols of different size distributions. Aerosols with a significant coarse mode, such as mineral dust or sea salt, have Angstrom coefficient values close to 0, whereas aerosols dominated by fine-mode particles, such as particles from fossil fuel combustion and biomass burning, have Angstrom coefficients higher than 1. Simultaneous information on AOT and Angstrom coefficients can thus be used to estimate the atmospheric load of mineral dust containing large amounts of coarse particles. For a long time, this retrieval method was restricted to surfaces with low albedo and in particular to oceanic surfaces. As an alternative, indicators of the presence of absorbing aerosol have been developed based on measurements in the UV (Herman et al., 1997; Torres et al., 1998) or in the infrared (Legrand et al., 1994, 2001). These aerosol indices have been used widely, in particular for mineral dust source identification (i.e., Prospero et al., 2002). Sensors of novel generation, with spectral capabilities, or additional types of measurements (i.e., polarization, several view angles), have increased the capability to characterize the different aerosol types and to retrieve AOT over land surfaces significantly. Nevertheless, AOT retrieval from satellites is limited to clear-sky conditions, which may constitute a bias for meteorological

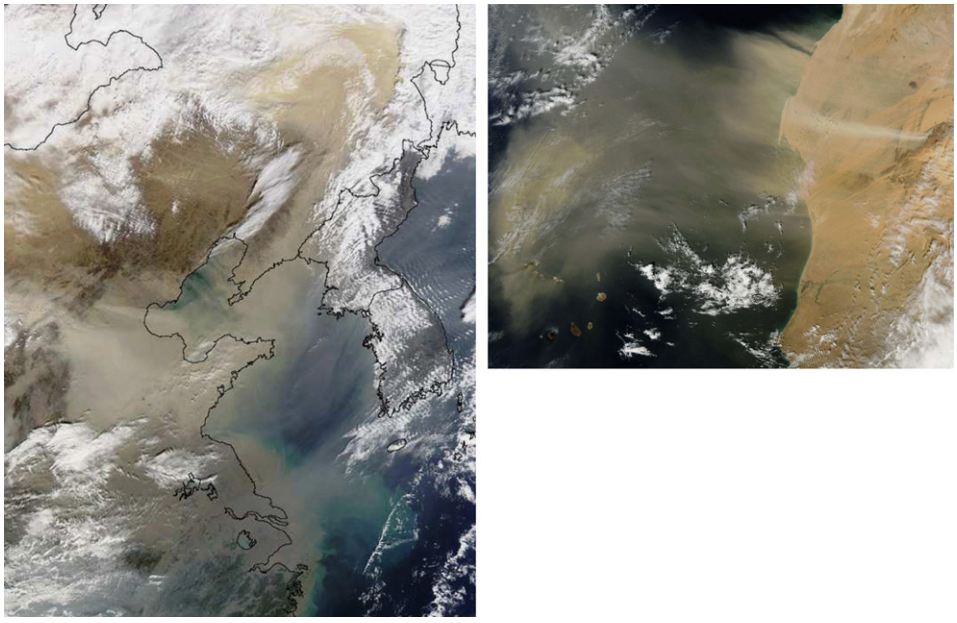

Figure 2 Visible MODIS (Moderate Resolution Imaging Spectroradiometers) images of dust plumes over the Yellow Sea (left) and downwind of North Africa.

analyses. All main techniques to retrieve AOT are based on a radiative transfer calculation applied to a limited number of aerosol 'models' (microphysical, i.e., size distribution, refractive index, or optical, i.e., AOT, single scattering albedo, asymmetry factor) including mineral dust. Both the aerosol model and the AOT are determined as the best fit of the calculation onto the observations. The higher the number of constraints on the fit the more accurate the result. Because AOT is the result of such retrievals, it may differ depending on the instrument and the algorithm. This implies that specific validations with ground-based AOT measurements and intercomparison between products are essential. Providing ground-based measurements of AOT is one of the main motivations of the international network of sunphotometers AERONET (AErosol RObotic NETwork; http://aeronet.gsfc.nasa.gov/) established by NASA and the French national research agencies (Centre National d'Etudes Spatiale (CNES); Institut National des Sciences de l'Univers, Centre National de la Recherche Scientifique (CNRS-INSU)). Finally, temporally averaged AOT can also vary from one sensor to the other depending on the temporal sampling. Typically, satellites in geostationary orbits provide higher sampling rates than polar-orbiting satellites, but for limited regions. As an example, Cakmur et al. (2001) indicated that at some periods, the presence of clouds limits the availability of AVHRR retrievals over the North Atlantic Ocean, making an accurate estimation of the monthly average AOT impossible and a proper investigation of the month-to-month variability difficult.

The first global pictures of AOT have been established based on observations from the AVHRR on board NOAA polar-orbiting satellites. Primarily designed to monitor the Earth's weather and in particular the clouds, AVHRR satellites were also part of the 'Early Earth Observing System (EOS) Pathfinder Data Set Activity' initiated in 1990 by NOAA. The retrieval algorithm assumes a simple power-law size distribution (Junge function) and aerosol optical properties of nonabsorbing aerosol (Stowe et al., 1997). Despite the poor relevance of this aerosol model to represent mineral dust properties, the global maps of AVHRR AOT clearly pointed out significant AOTs downwind of mineral dust sources (Husar et al., 1997). Similarly, the European Meteosat satellites, initially dedicated to weather monitoring, have also been used to investigate atmospheric aerosols. Moulin et al. (1997) improved an initial algorithm (Tanré and Legrand, 1991) to retrieve AOT specifically due to African dust outbreaks based on Meteosat imagery. Because of their geostationary orbit and geographical position (centered on Africa), Meteosat imagery does not provide a global coverage but allows very good temporal sampling over the north tropical Atlantic Ocean. The recent Moderate Resolution Imaging Spectroradiometers (MODIS) onboard the Terra (since 1999) and Aqua (since 2002) satellites from the NOAA EOS allows the retrieval of the AOT at a global scale with a high level of confidence over both ocean (Remer et al., 2005) and land (Levy et al., 2007). The latest version of MODIS AOT retrieval algorithm (Collection 5) has been used to propose global aerosol climatology (Remer et al., 2005).

Similar data have been used to produce the global maps of mean AOT and associated Angström coefficient over the period 2001–05 (**Figure 3**). The main features of this global picture do not differ much from those discussed by Husar et al. (1997) using AVHRR AOT or Remer et al. (2005). The mean AOTs are clearly higher in the Northern Hemisphere than in the Southern Hemisphere. Over the oceans, large plumes of high AOT are clearly seen downwind the main arid regions of the world, that is, North Africa and the Arabian Peninsula. An extensive plume is also visible downwind of Asia but with lower AOT. These plumes decrease in intensity as a function of greater distance from the coast. The North Atlantic plume extends from the African coast to the Caribbean, whereas the area of large AOT to the south of the Arabian Peninsula does not develop as far. The less intense Asian plume appears to extend from the Asian coast almost to the west coast of North America. The location of these dust plumes compared to the location of the arid and semiarid regions of the world suggests that mineral dust emissions can be responsible for such high AOT. The low Angström coefficients in the aerosol plumes over the North Atlantic Ocean indicate the presence of coarse aerosols and thus reinforce the hypothesis that mineral dust has dominated the AOT in these regions. However, strong AOTs are also observed in regions that are not located downwind of mineral dust source regions. The high AOT observed over the Gulf of Guinea or in Africa south of the equator can reasonably be attributed to biomass

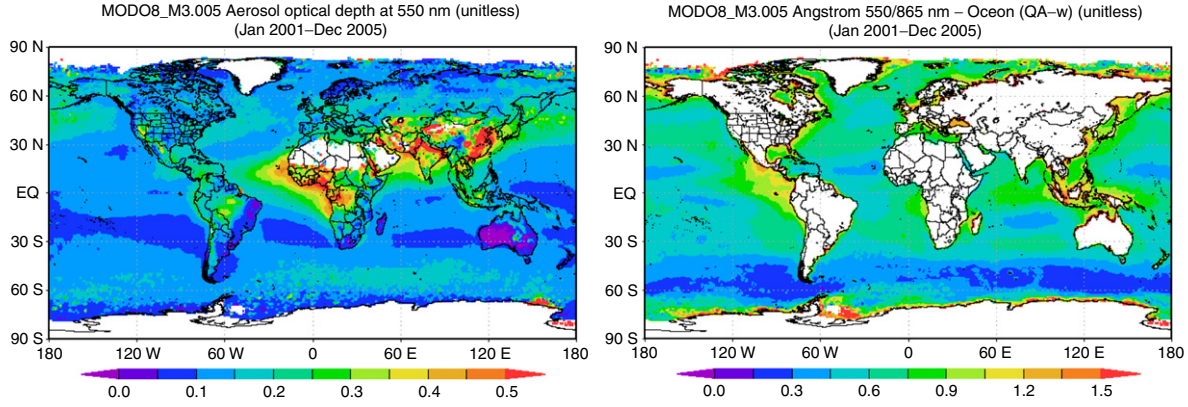

Figure 3 Global mean (2001–05) MODIS (collection 5) Aerosol Optical Depth at 550 nm and Angstrom coefficient (550–865 nm) (analyses and visualizations produced with the Giovanni online data system, developed and maintained by the NASA GES DISC).

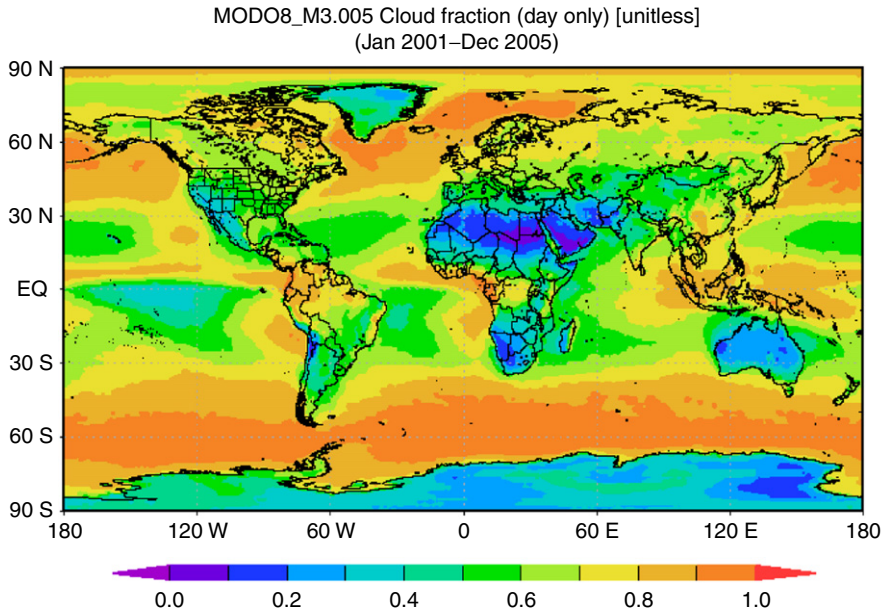

Figure 4 Global mean (2001–05) MODIS (collection 5) day-time cloud fraction (%) (analyses and visualizations produced with the Giovanni online data system, developed and maintained by the NASA GES DISC).

burning aerosol. Once again, this tends to be confirmed by the high Angström coefficient in these regions. Although the west coast of Africa appears to be embedded in a large area of high AOT, an examination of the Angström coefficient can distinguish the presence of different aerosol types. From the Angström coefficient, it can be seen that coarse dust aerosol predominates north of the equator whereas fine aerosols, presumably due to biomass burning, predominates along the west coast of southern Africa. High AOTs are observed over Asia, in particular over a large area including Beijing ($\sim 30^\circ$ N and 120° E). The Taklamakan Desert also exhibits high AOTs. However, over the North Pacific Ocean, the AOTs are not as intense as over the North Atlantic Ocean. In addition, the Angström coefficient does clearly indicate a dominance of coarse particles. This is partly explained by the fact that Asia is also the source of large amount of fine anthropogenic aerosols. As a result, mineral dust transported from Asian deserts is commonly mixed with fine, pollution-derived aerosols. Such a mixing between mineral dust with aerosols from diverse sources (volcanic, sea salt, and so on), but in particular with anthropogenic aerosols (sulfates, carbonaceous aerosols, etc.), was observed in the marine boundary layer over the Sea of Japan during the ACE-Asia campaign (Bates et al., 2004). Zhang et al. (2005) analyzed aerosol compositions during an extremely intense dust storm that affected Beijing on March 20, 2002, and concluded that dusty air often contains higher levels of pollutants than nondusty air. However, the shape of the plume suggests relatively intense aerosol transport between 30° N and 60° N and eastward of 180° E or further. This pathway is comparable to one identified from a trajectory analysis (Merrill et al., 1989) performed to investigate the transport of Asian dust to Midway Islands ($28^\circ 132$ N–$177^\circ 212$ W), a station in the SEAREX network (Sea/Air Exchange Program; Uematsu et al., 1983). Consistently, during the ACE-Asia campaign, it was found that transport of Asian aerosols can reach Alaska where deposition of particles enriched in crustal elements was detected (Cahill, 2003). Another factor that may affect the retrieval downwind of northern Asia, compared to North Africa, is a higher cloud cover (**Figure 4**). The persistence of clouds in the Southern Hemisphere (**Figure 4**) was also found to limit the satellite detection of mineral dust plumes. As an example, Gasso and Stein (2007) analyzed a case of long-range transport of dust originating from Patagonia and advected over the southwestern Atlantic Ocean. They demonstrated that cloudy conditions associated with the lack of good viewing geometry did not allow an automatic detection of such transport events. They also argued that even in clear-sky conditions, because they are short-lived events (a few hours), mineral dust transport from Patagonia cannot be properly captured and quantified using satellite observations only.

11.5.2.2 Main Seasonal Patterns

Mineral dust emissions generally exhibit a marked seasonal cycle, which is expected to impact the dust atmospheric content in transport regions. This is illustrated by the seasonal map of AOT and Angström coefficient in the year 2001 (**Figure 5**). AOT appears as very high during the spring (January–February–March) and the summer (April–May–June) in the Northern Hemisphere, consistent with the fact that dust emissions are at a maximum in this season over North Africa (i.e., Laurent et al., 2008) and eastern Asia (i.e., Laurent et al., 2008). However, even within a seasonal cycle, it is generally difficult to extract a clear and 'pure' dust signature from the Angström coefficients over Asia. In the summer, AOT values are still high over the North Atlantic but the dust plume tends to be shifted to the north and reaches the Caribbean, whereas in the spring, it reaches the northern part of South America. This seasonality of the AOT plumes is in agreement

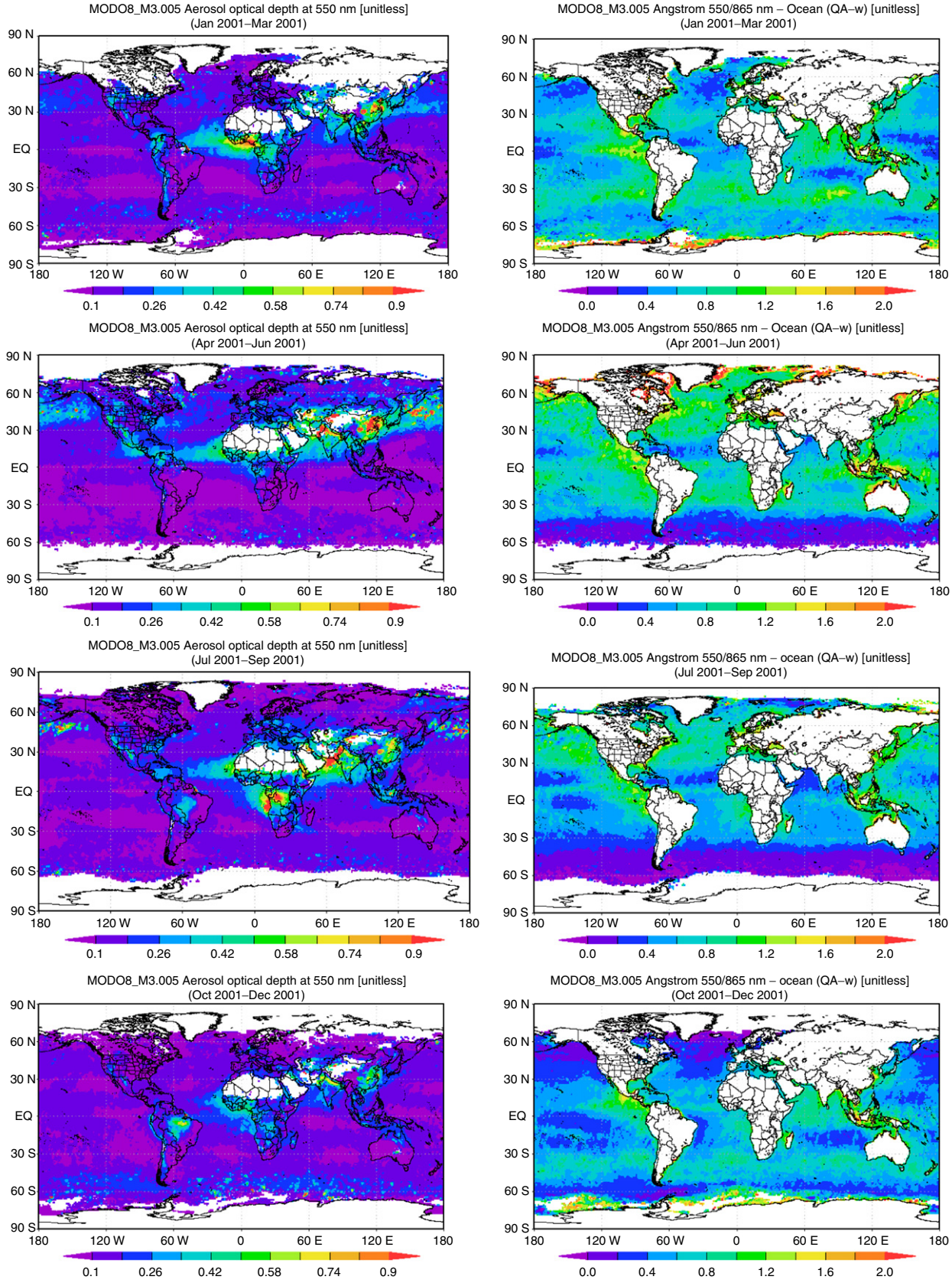

Figure 5 Seasonal average MODIS Aerosol Optical Depth at 550 nm and Angstrom coefficient (550–865 nm) for the year 2001 (analyses and visualizations produced with the Giovanni online data system, developed and maintained by the NASA GES DISC).

with the maxima of dust concentrations measured at the surface in Barbados in summer (Prospero and Nees, 1977) and in French Guyana in winter (Prospero et al., 1981a, b), as further described in Section 11.5.3.2. In summer, high AOTs are observed downwind of the Arabian Peninsula, associated with low Angström coefficients. This period corresponds not only to the maximum of dust emissions from Arabian deserts, as derived from IR satellite imagery (Deepshikha et al., 2006), but also to a high level of dust storm activity in southwestern Asia (Iran, Afghanistan, Pakistan, and northwestern India) (Middleton, 1986). In the Southern Hemisphere, the only region with very high AOTs is located in southern Africa and corresponds to export of aerosols from biomass burning, as revealed by high Angström coefficients.

11.5.2.3 Transport Routes

An examination of the average AOT picture tends to mask the fact that long-range dust transport results from a collection of individual events, some of which may not be sufficiently intense and frequent to be properly detected by satellite imagery. However, whatever their origin, dust transport events usually follow specific pathways determined by synoptic meteorological conditions. These pathways, determined mainly from a synthesis of reported individual events, are illustrated in Figure 6. Although the major dust plumes identified from Figures 3 and 4 are displayed, in particular the dust plumes originating from North Africa, the Arabian Peninsula and from northeastern Asia, additional transport pathways are also reported. Some of them correspond to continental transport that may not be correctly retrieved from satellite imagery. This is typically the case for the transport of mineral dust from central Asia. Over the North Pacific Ocean, in addition to the northern trajectory corresponding to the AOT plumes attributed to Asian mineral dust discussed earlier, a southern trajectory of Asian dust is reported. This pathway corresponds to the main trajectory of Asian dust toward Korea, known locally as 'yellow sand' events. Based on meteorological records in Seoul (Korea) between 1915 and 2000, Chun (2000) estimated a frequency of Asian dust transport toward Korea of 4 day per year. The annual number varies significantly from one year to the other (from 0 to 14) but occurs mainly during the spring, with occasional events during the winter. Dust transport from Arabian deserts can be transported not only to the south of the Arabian Peninsula, as observed on the AOT picture, but also to India, passing through the northwestern part of the peninsula with a curved trajectory over land. Other pathways correspond to transport from sources that are not very intense or frequent, such as those from Australian, South African, and South and North American deserts. Regarding their intensity, most of these additional transport pathways are generally considered to correspond to medium-range transport. However, they still can be responsible for long-range transport of detectable amounts of dust. As an example, and as already mentioned, Gasso and Stein (2007) identified an event of mineral dust transport from Patagonia toward the southwestern Atlantic Ocean capable of reaching the Ocean adjacent to Antartica. Finally, mineral dust is recorded in arctic regions both in the North and South Hemispheres. Biscaye et al. (1997) showed that mineral dust collected in present-day Greenland ice sheet originates mainly from Asian Deserts, whereas Patagonia (South America) is considered as the main present-day source of mineral dust in Antarctic ice-cores.

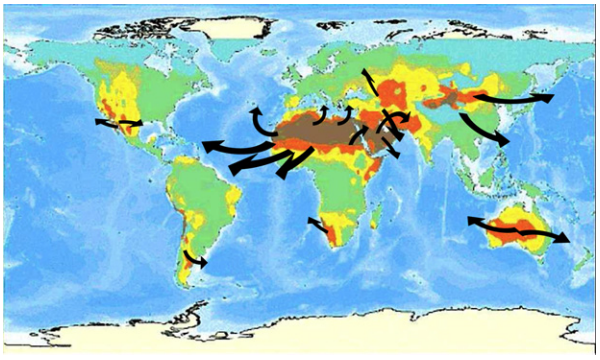

Figure 6 Main transport pathways of transport of mineral dust. Adapted from Meigs, P., 1953. World distribution of arid and semi arid homoclimates. In: Reviews of Research on Arid Zone Hydrology. UNESCO, Paris, pp. 203–209 and Coudé-Gaussen, G., 1984. Le cycle des poussières éoliennes désertiques actuelles et la sédimentation des loess péridésertiques quaternaries. Bulletin des Centres de Recherches Exploration Production Elf-Aquitaine 8, 167–182.

11.5.3 Meteorological Processes Associated with Dust Long-Range Rransport Pattern and the Seasonal Cycle

Long-range transport of mineral dust is controlled not only by the location of the dust sources and the temporal variability of the emissions, but also by meteorological conditions allowing or inhibiting dust export from source regions, its advection in specific directions, and its removal from the atmosphere. The main processes of long-range transport of Saharan and Asian dust have been derived initially from meteorological analysis of case studies identified from measurements of mineral dust concentrations and then further investigated based on satellite observations. This has provided a conceptual understanding of these processes and a quantification of the intensity and frequency of the dust long-range transport events. On these two points, the continuous efforts since the 1970s and the tremendous contributions of Prospero and collaborators from the Rosenstiel School of Marine and Atmospheric Science (Miami, FL, USA) must be acknowledged. Much of the work of this group, especially their findings on the vertical distribution of dust, have been confirmed recently, thanks to the development of ground-based and spaceborne lidar detection systems.

11.5.3.1 Asian Dust Transport Toward the North Pacific Ocean

Although global maps of AOT show a moderately intense aerosol plume downwind of Asia, long-range transport of mineral dust into the Pacific Ocean was observed in the 1980s from surface dust concentrations in the central (Duce et al., 1980) and north Pacific Ocean (Uematsu et al., 1983). In the

framework of the SEAREX program, weekly aerosol sampling has been conducted at several stations on islands of the north Pacific Ocean between ~0–50° N and 150° E–150° W from 1980 to 1983. A complete analysis of these measurements can be found in Prospero et al. (1979). Annual mean concentrations exhibit a gradient of decreasing dust from north to south, with concentrations of the order of 1 $\mu g\,m^{-3}$ at the northernmost station, down to less than 0.1 $\mu g\,m^{-3}$ around the equator. Despite a large year-to-year variability, all stations consistently recorded pulses of high dust concentrations in the spring and a moderate peak in the fall. This seasonal cycle is very similar to the one of the Asian dust emissions. Using synoptic weather reports, Sun et al. (2001) estimated that 90% of the dust emitted from Chinese deserts occurs from March to May. Based on a six year simulations, Laurent et al. (2006) confirmed that dust emissions are at a maximum in the Taklamakan and Gobi deserts in the spring. However, they found a secondary dust emission maximum in November, mainly due to the contribution of northeastern arid areas (i.e., Inner Mongolia, and the Horqin, Otindaq, and Hulun Buir deserts). The contribution of these deserts to long-range dust transport in the fall is further confirmed by the analysis of dust isotopic signatures in Greenland (Bory et al., 2003). This suggests that dust emission variability is the main factor controlling the variability of surface concentrations. This hypothesis is reinforced by the fact that the year-to-year variability of dust surface concentrations also tends to follow the variability of the dust storm records (Prospero et al., 1979). The meteorological processes responsible for Asian dust transport over the north Pacific Ocean have been thoroughly investigated by Merrill et al. (1989) using back-trajectories analyses to the dust events detected by the SEa/Air EXchange program (SEAREX) network. The typical scenario they propose for spring dust events corresponds to dust emission events from Asian deserts associated with the passage of vigorous cold fronts. The dust plumes follow an almost direct and descending trajectory toward the central and south North Pacific Ocean, reinforced by the trade winds. Transport from sources to the central Pacific Ocean was found to require 8 to 14 days with path lengths typically 10 000–15 000 km. Precipitation was identified as the ultimate factor controlling long-range transport. Typically at a given station, the highest concentrations are measured during the longest dry periods, and the station with the highest precipitation rate exhibited the lowest mean and peak concentrations. From this trajectories analysis, it was expected that dust would be distributed from the surface to as high as 8–10 km, but spring transport was expected to take place primarily in the mid-troposphere. The altitude at which Asian dust can be injected depends to a greater extent on the considered desert from which the dust originated. Based on a compilation of 40 years of record over China, Sun et al. (2001) confirm the predominant role of frontal systems and of the Mongolian cyclonic depression in Asian dust emissions. Because of a complex topography (a basin surrounded by high mountains) inducing a specific local circulation in the Tarim Basin, dust raised from the Taklimakan Desert is commonly entrained to elevations of >5000 m and can be transported long distances (~5000 km away) by the westerly jet (Sun et al., 2001). However, dust emitted from the Gobi desert, mainly by synoptic-scale cyclones, is dominantly (90%) located below 3000 m and thus subjected less frequently to long-range transport. However, it can occasionally be entrained in the middle troposphere and then efficiently transported over long distances by the westerly jet stream (Sun et al., 2001).

Such a difference in the altitude of transport may explain complex vertical structures as they have been observed over Japan by ground-based lidar. A two-layer structure was identified at 2 and 6 km, corresponding, respectively, to dust transported from the Taklamakan Desert and from the Gobi Desert (Kobayashi et al., 1985). Asian dust transport over the north Pacific Ocean has been specifically investigated in the framework of the PACific Dust Experiment (PACDEX) that took place from March to May 2007 (Huang et al., 2008). A statistical analysis of the vertical structure of mineral dust associated with long-range transport has been conducted using ground-based (MicroPulse Lidar, MPL), spaceborne (Cloud-Aerosol Lidar and Infrared Pathfinder Satellite Observation (CALIPSO)) lidar systems. This study confirms the frequent occurrence of two-layer structures that were again interpreted to be from different dust events or dust sources. CALIPSO observations show that dust layers originating from the Gobi Desert can expand up to 8 km high, that is, much higher than suggested by Sun et al. (2001). With such a dust layer depth, long-range transport becomes possible both in the lower and the upper troposphere (Huang et al., 2007). The dust vertical distribution was also investigated using several years of measurements from the Stratospheric Aerosol and Gas Experiment II (SAGE II) onboard the Earth Radiation Budget Satellite (ERBS) (Zhu et al., 2007). The mean vertical profile during the dust season (March–April–May from 1981 to 2001) is characterized by a complex multilayer structure that still can be explained by the superposition of dust plumes originating from different source regions. Dust originating from the Taklamakan Desert is suspected to be more efficiently transported over long distances because of extremely high injection altitudes. As an illustration, a 'full circuit around the globe' has been recently identified and investigated (Uno et al., 2009). CALIPSO measurements, trajectory analyses and tridimensional dynamic simulations have been combined to study a dust storm that occurred in the Taklamakan Desert in May 2007. Dust was found to be uplifted in the free troposphere as high as 8–10 km. The dust plume was then transported more than one full circuit around the globe in about 13 days. At the second passage of the dust plume over the northwestern Pacific, the subsidence of a large-scale high-pressure system finally caused its descent into the lower troposphere. Such events could not have been detected without the input from the spaceborne lidar system.

Long-range transport of Asian dust is controlled largely by the characteristics of the Asian dust emissions. The temporal variability of the dust emissions controls the seasonality and interannual variability of the long-range transport. The location of the dust sources and the meteorological conditions prevailing during dust emission largely impact the altitude at which mineral dust is injected and thus the intensity and extension of the associated long-range transport. Precipitation patterns along the transport path act mainly as an inhibitor or ending factor for the transported dust plumes.

11.5.3.2 North African Dust Transport Toward the North Tropical Atlantic Ocean

Long-range transport of mineral dust from North Africa is the most intense and the best documented in the world. As discussed above, the trans-Atlantic transport of Saharan dust was documented for the first time thanks to chemical and mineralogical analyses of daily aerosol samples collected on Barbados in the Caribbean, as part of a search for cosmic dust (Delany et al., 1967; Prospero, 1968). In addition to an unambiguous demonstration of the African origin of the dust, this monitoring also showed the seasonal character of the African dust transport to the Carribean. Since that early study, African dust transport has been documented every year with a maximum in the summer (Figure 7). The average dust concentration during the dust season is on the order of 10 μg m^{-3} and about an order of magnitude lower the rest of the year (Prospero, 1968). A similar seasonal cycle was observed for dust measurements made further north on Bermuda and in Miami (FL, USA) (Prospero and Nees, 1986; Arimoto et al., 1995). Although such concentrations and the estimated duration of the dust transport from Africa to western Atlantic Ocean (5–7 days) indicate efficient sediment transport, maximum dust flux does not always coincide with the maximum of dust emission in Africa. A comparable aerosol monitoring program was conducted over two years in Cayenne (French Guyana), 10° south of Barbados (Prospero et al., 1981a, b). The maximum monthly mean concentrations in Cayenne were slightly higher

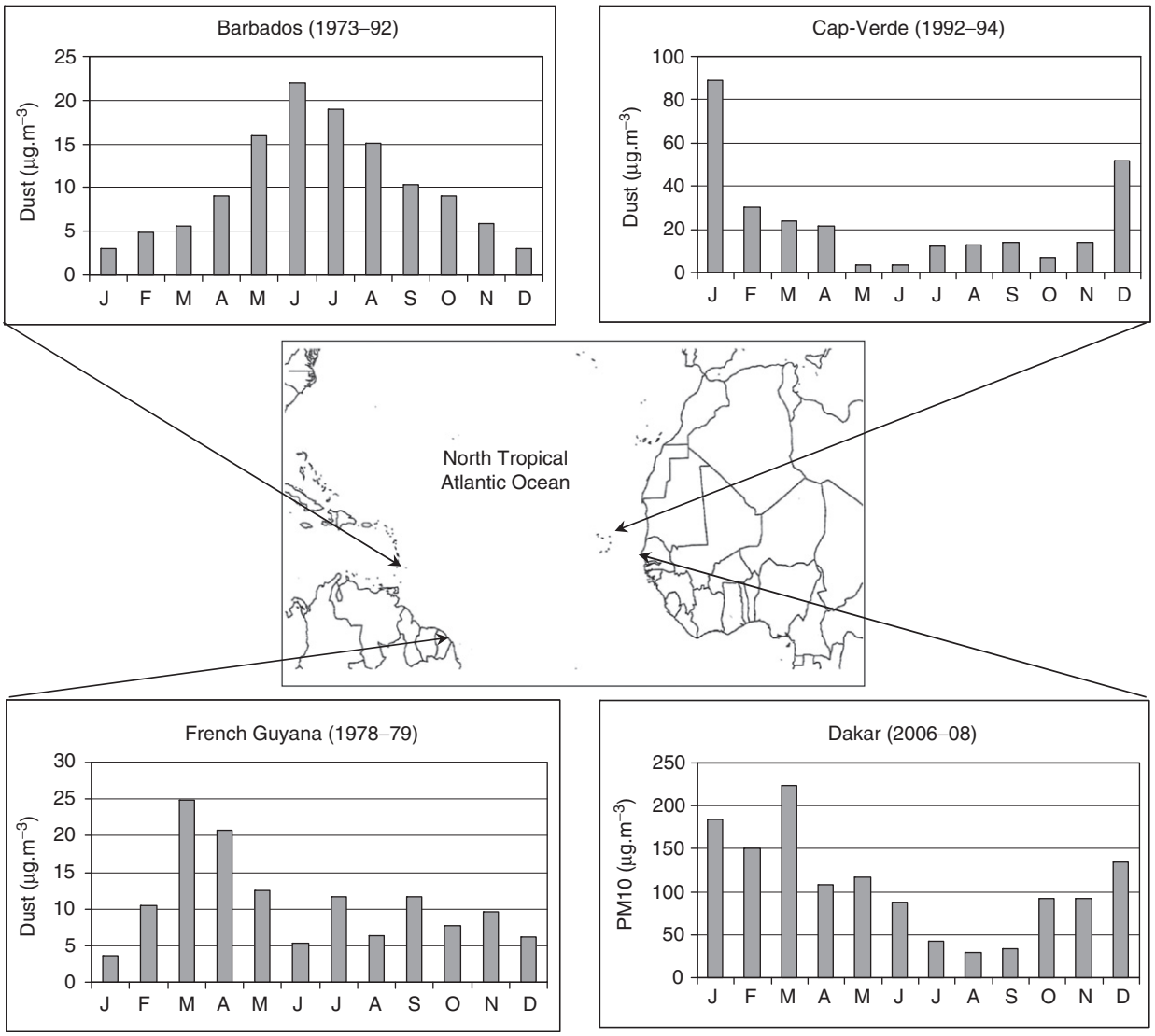

Figure 7 Typical seasonal cycle of the monthly mean dust concentrations or PM_{10} concentration. Barbados and French Guyana: data from Prospero, J.M., Carlson, T.N., 1981. Saharan air outbreaks over the tropical North Atlantic. Pageoph 119, 677–691; CapeVerde: data from Chiapello, I., Bergametti, G., Gomes, L., et al., 1995. An additional low layer transport of Sahelian and Saharan dust over the north-eastern tropical Atlantic. Geophysical Research Letters 22, 3191–3194, and Dakar: data derived from Marticorena, B., Chatenet, B., Rajot, J.L., et al., 2010. Temporal variability of mineral dust concentrations over West Africa: analyses of a pluriannual monitoring from the AMMA Sahelian Dust Transect. Atmospheric Chemistry and Physics Discussion 10, 8051–8101.

(23–28 μg m^{-3}) than on Barbados (15–18 μg m^{-3}) (**Figure 7**), with a maximum dust concentration recorded in March, that is, at the period when dust activity is at the maximum in North Africa (Laurent et al., 2008). African dust transport events have also been recorded in the Amazon basin during this period of the year (Swap et al., 1992). Closer from the African coast, dust concentrations measured in the Cape Verde Islands (16° N; 22° W), 500 km west from the coast of Senegal, also exhibit a strong seasonality with a maximum in winter (December–January) and a minimum in summer (Chiapello et al., 1995). The monthly mean concentrations, at the dust maximum, range between 50 and 90 μg m^{-3} and are lower than 10 μg m^{-3} in summer. For sake of comparison, the monthly mean concentrations of PM_{10} (particulate matter with diameter smaller than 10 μm) measured in Dakar (Senegal) (Marticorena et al., 2010) have also been plotted on **Figure 7**. Since the whole dust size-spectrum is not collected, PM_{10} concentrations provide a lower limit indication of dust concentrations. The maximum monthly PM_{10} concentrations range from 225 μg m^{-3} in March to about 30 μg m^{-3} in August. The maximum concentration is observed in March and is due to Saharan dust transport. The lowest concentration is recorded during the Sahelian wet season (July–August–September). Mineral dust concentrations in all these locations show a consistent east to west gradient, with concentrations decreasing as a function of the distance to the African coast, but different seasonal cycles and in particular differences in the period of dust concentration maximum. These differences can be explained either by the fact that they are affected by dust originating from different sources or following different transport pathways.

There have been some recent studies on dust emission variability over west Africa. Based on pluri-annual simulations, Laurent et al. (2008) showed that simulated and observed dust emissions over the entire Sahara Desert exhibit a seasonal cycle characterized by a maximum in the spring and a minimum in the fall. However, Laurent et al. (2008) also found that dust emissions from the West Sahara are highest during the summer, consistent with the observed reduction of horizontal visibility at this time (Mahowald et al., 2007). Marticorena and Bergametti (1996) also indicate that the seasonality of the dust emissions over the western Sahara was associated with a change in the location of the source region. The summer dust emission corresponds to a southwestern shift of the dust sources between spring and summer, with a major contribution from dust sources located in northern Mauritania and Mali during the summer. In addition to these Saharan sources, mineral dust can be emitted from the Sahelian region by the passage of convective systems during the summer (Marticorena et al., 2010). Sahelian dust could thus be injected at high altitude (>10 km) by the deep convection and thus contribute to summer long-range transport across the Atlantic Ocean. Recent study of soils from the Canary Islands have demonstrated that dust from the Sahel can be transported at considerable distance northward (Muhs et al., 2010).

In addition to seasonal differences in the dust emission location and intensity (**Figure 5**), the direction of the African dust plume shifts to the north from winter to summer. This change in the direction in the dust plume is related to the south to north displacement of the Intertropical Convergence Zone (ITCZ) in summer. In winter, much of North Africa is under the influence of the Harmattan, a northeasterly flow extending toward the Gulf of Guinea. The more southerly winter position of the ITCZ allows dust transport to the central and southern part of the north Atlantic Ocean. This transport pattern at the period where dust emissions are maximum explains the high African dust concentrations measured in the Cape Verde Islands and the northern part of South America. In the summer, the ITCZ is shifts northward. Dust injected into the Saharan Air Layer (SAL) by the Harmattan winds is thus lifted above the monsoonal flow. The flow turns southwestward over the north Atlantic Ocean and dust can be efficiently transported by the northeast trade winds as well as at higher altitudes by the SAL. This latitudinal shift in the position of the African dust plume is thus the main factor explaining the opposition in the seasonal cycle of surface dust concentrations measured in Barbados and French Guyana. The variability of the Saharan dust outbreaks and of the associated synoptic meteorological fields has been recently investigated using MODIS imagery from 2003 to 2007 (Huang et al., 2010). This analysis is limited to relatively intense dust transport events because dust outbreaks, in this study, are defined by AOTs exceeding the 5-year mean AOT by one standard deviation. The pathway of these dust outbreaks from the west African coast toward the north tropical Atlantic Ocean was investigated by back and forward trajectories and by distinguishing different initial direction sectors along the west African coast: a northern direction (20–30° N), central direction (10–20° N), and south direction (0–10° N). As expected, most of trajectories of the dust events leaving the African coast in the northern direction travel to the West Indies during the summer. Carlson and Prospero (1972) suggested that the summer African dust transport events in the SAL are associated with African easterly waves (AEW). The frequency of intense African dust outbreaks derived from the analysis of satellite aerosol retrieval has been estimated to be 6 days per month, that is, consistent with the periodicity of the AEW (Huang et al., 2010). About half of the outbreaks in the northern sector reach latitudes north of 20°N along the east coast of USA (Prospero, 1999). Transport of dust to the Gulf of Mexico and the southeastern USA has also been documented (Perry et al., 1997). Several African dust transport events in the eastern USA in the summer (1991–93) have been reported, reaching as far west as Texas, although most of them occurred in Florida. The seasonal modulation, the frequency, and the extent of these events depends on meteorology, with a key role being played by the semipermanent Bermuda high pressure cell with clockwise transport from the eastern coast of Florida to the Gulf of Mexico and southern USA (Perry et al., 1997)). Whatever the direction, the life time of the dust outbreaks is on the order of 7 days, with extreme durations of 12 days and a tendency to have shorter life time in the southern direction. These spatial and temporal patterns explain the difference in the seasonal cycle recorded in Barbados and French Guyana (**Figure 7**) and the seasonality of the PM_{10} concentration in Dakar but do not explain the seasonal cycle of the dust concentrations in Cape Verde Islands.

This seasonal change in the latitudinal position of the North African dust plume is associated with a change with the altitude of dust transport. During winter, easterly winds are restricted to a relatively shallow layer below 1.5–3 km,

whereas at higher altitudes westerly winds prevail (Chiapello et al., 1995). Saharan dust is thus transported within the SAL above the trade winds inversion (Prospero and Carlson, 1981). Aerosol vertical distribution and AOT have been monitored in Senegal on the northwest African coast from January 2006 to September 2008 (Léon et al., 2009). The maximum AOT is observed in summer and corresponds to a maximum in the top altitude of the transported aerosol layer (up to 6 km) due to the presence of the SAL, between 2 and 6 km. An additional low-level layer of increasing depth is observed from late summer to fall. The average vertical distribution of summer dust derived from pluriannual observations of the spaceborne lidar CALIPSO over the African coast and the eastern tropical Atlantic Ocean is characterized by an upper altitude of about 5 km (Huang et al., 2010), consistent with the vertical distribution derived from aircraft aerosol sampling (Carlson and Prospero, 1972). From the west African coast to the Caribbean the SALs top altitude decrease from 5 to 3 km (Huang et al., 2010). The aerosol profiles measured during several dust events sampled during the PRIDE experiments showed consistent but quite higher altitudes for the top of the SAL (Reid et al., 2003a). The mean altitude of the base of the dust layers determined from CALIPSO observations vary from about 1–2 km along the African coast to 0.5 km over the ocean (Huang et al. 2010).

Vertical aerosol distribution monitoring in Senegal shows that severe dust storms are systematically observed in spring (March) but with a lower vertical development and a stronger impact on the ground-level mass compared to summer (**Figure 8**). The pluriannual analysis of CALIPSO data shows that during the winter, the top of the dust layer is lower than in summer. It is about 3–4 km altitude over Africa and 2–3 km over the Atlantic Ocean, whereas the bottom can be as low as 200 m in central Atlantic Ocean (Huang et al., 2010). Surprisingly, the dust layer rises again west of 40° W, with the highest lifting being observed between 60 and 80° W, over the Amazon basin, probably due to convection over South America.

This seasonal shift in between winter and summer explains the anticorrelation of the surface concentrations and AOTs measured in Cape Verde and in Dakar (Senegal) (**Figures 7** and **8**). Low layer transport is responsible for the winter maximum in the surface concentration, whereas the summer transport in the elevated SAL explains the summer maximum of the AOT. This summer transport in the SAL favors the long-range transport of African dust toward the Atlantic Ocean and Barbados and thus explains the seasonal cycle of the measured surface concentrations (**Figure 7**) and AOT (**Figure 8**). The seasonal cycles of AOT associated with mineral dust measured Cape Verde and Barbados are similar, suggesting that they are affected by the same transport process.

The role of precipitation for terminating these dust transport events is seen both in the regional climatology and at the scale of individual events. As a general trend, the southern extension of the African dust outbreaks is thought to be limited by an efficient wet removal in the active ITCZ (Junge, 1979). As an illustration of the seasonal shift of the ITCZ, **Figure 9** shows a MODIS image of the cloud fraction in winter and summer 2001. In the winter, over the north tropical Atlantic Ocean, the high cloud cover region associated with the ITCZ is located below 5° N, whereas in summer it is shifted northward up to 10–15° N. Looking at the position of the cloud fraction and of the AOT, it can

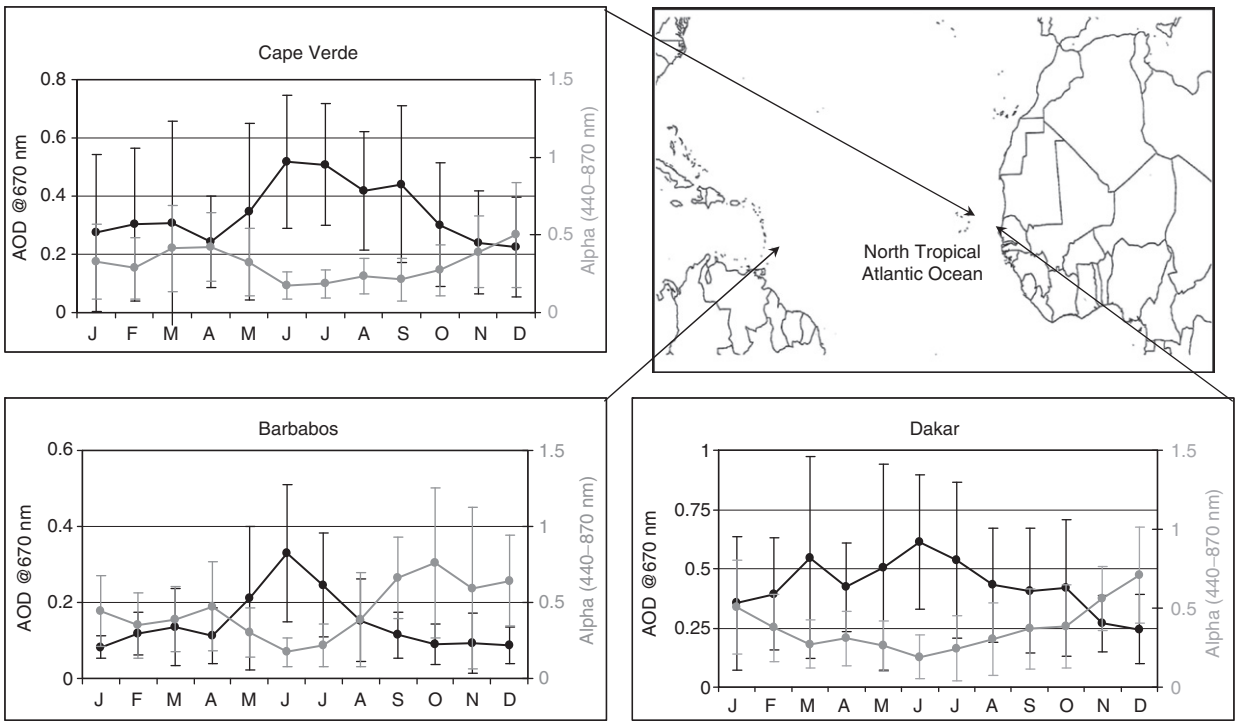

Figure 8 Monthly mean Aerosol Optical Depth at 670 nm and Angstrom coefficient (Alpha) between 440 and 870 nm from 1996 to 2007 measured with the AERONET sunphotometers.

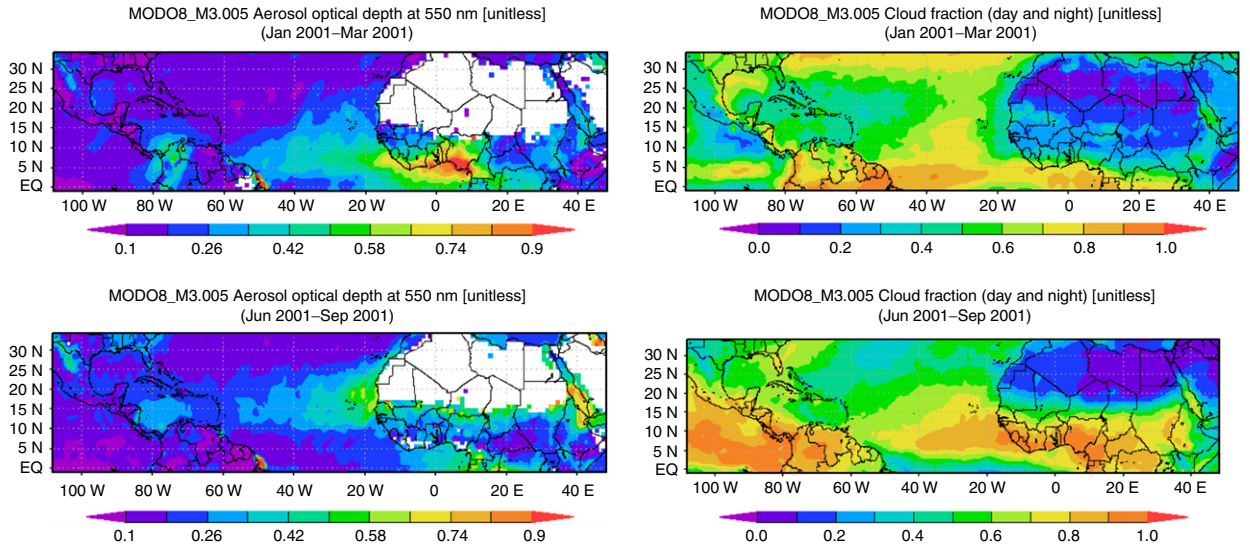

Figure 9 Winter (January–February–March) and summer (July–August–September) average MODIS Aerosol Optical Depth at 550 nm and cloud fraction for the year 2001 (analyses and visualizations produced with the Giovanni online data system, developed and maintained by the NASA GES DISC).

be seen that the cloud pattern and its seasonal shift match with the southern limit and the seasonal shift of the dust plumes. At the event scale, pulses of African dust have been recorded over the Amazon Basin in April and May 1987 that were associated with major wet-season rains (Swap et al., 1992).

To summarize, the spatial distribution and temporal pattern of mineral dust transport from North Africa over the North Atlantic Ocean results from the combination of factors including the temporal variability of the dust emissions and source location, the temporal variability of the synoptic conditions prevailing over the Atlantic Ocean and the absence of precipitation along the transport paths.

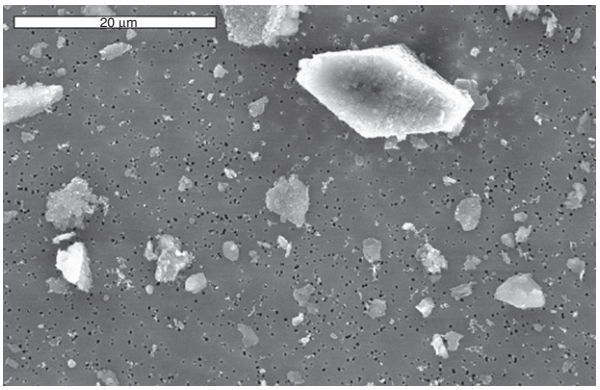

Figure 10 Scanning electron microphotogram of mineral dust particles.

11.5.4 Properties of Transported Dust

The size-resolved concentrations, composition, and shape of mineral dust particles are the physical and chemical properties (independent of concentration) underlying their various climatic and environmental impacts. These characteristics determine the optical properties (scattering and absorption coefficients), solubility and hygroscopicity of mineral dust, which control the impact of dust on the global radiation budget, marine productivity and cloud formation and reflectance, respectively.

The physico-chemical properties of mineral dust at the points of emission depend on the mineralogy and the dry size distribution of the source sediments and the strength of the wind friction velocity (Laurent et al., 2008). At the source, mineral dust is commonly composed of quartz, feldspars, micas, carbonates, clay minerals, and iron oxides (Pye, 1987; Schutz and Sebert, 1987; Caquineau et al., 2002; Cheng et al., 2005). All these minerals have different crystalline structures, different water affinities, and different size distributions; therefore they have different optical and solubility properties, leading to different impacts (Sokolik and Toon, 1999; Journet et al., 2008). The number and mass size distribution of mineral dust extends over many orders of magnitude, both in concentration and in diameter range, which vary from fractions to tens of microns (d'Almeida and Schütz, 1983). The presence of a significant coarse mode (mass-median diameter of 3–5 µm) is a major feature of the mass size distribution of mineral dust. Dust particles can be irregular in morphology and surface roughness. A scanning electron micrograph of mineral dust particles collected over a polycarbonate substrate (**Figure 10**) illustrates the irregular morphology of typical dust.

Because of their complexity and variability, the observation of the variability of the physico-chemical properties of mineral dust remains a great experimental challenge, requiring the combination of multiple techniques. An example is provided by Reid et al. (2003b) with respect to the measurement of the coarse mode particle fraction of the size distribution. These authors compared various *in situ* sizing and remote

sensing inversion methods deployed during the PRIDE campaign in Puerto Rico to show that the difference in the volume-median diameter of the coarse fraction might be as high as 3 depending if aerodynamic or optical sizers are considered. Although highlighting the implications for numerical calculation of the dust direct radiative effect (the coarse mode fraction rules the mass extinction efficiency), and making recommendations for observational best-practices, Reid et al. (2003b) concluded that some level of uncertainty must be accepted in studying the sizes of mineral dust.

The knowledge of the initial properties of dust particles is not sufficient to predict their evolution during their atmospheric cycle. The size-resolved concentrations, composition, and shape are affected, directly or indirectly, by various processes intervening while particles are airborne. These include aggregation, coagulation, dry deposition, particle-water interaction, mineral alteration, wet scavenging in and below clouds, particle mixing, and condensation due to heterogeneous reactions in the dry and aqueous phases.

The current state of knowledge of physico-chemical properties of transported mineral dust mostly relies on measurements performed in the Caribbean, Mediterranean, and Japanese seas. These are intensive campaigns (ACE-2, SHADE, PRIDE, LBA-CLAIRE, MINATROC, ASTEX, PACDEX, ACE-ASIA, INTEX-B) or long-term observations such as those performed at Barbados since 1968 (Prospero, 1968). Despite the large body of observations, only a few attempts have been made to make systematic comparisons between the dust properties at the source and during or after transport (e.g., Formenti et al., 2003; Maring et al., 2003; Garrett et al., 2003; Trochkine et al., 2003).

The significant changes in coarse mode (mass-median diameter of 3–5 μm) particles, even after long-range transport, has been studied by various authors (Li-Jones and Prospero, 1998; Maenhaut et al., 1999; Formenti et al., 2001, 2003; Smolik et al., 2003; Maring et al., 2003; Garrett et al., 2003; Reid et al., 2003b, 2003c; Kuloglu and Tuncel, 2005; Marenco et al., 2006).

The first attempt of modeling the dynamics of the dust volume distribution during its export over the north eastern Atlantic Ocean is by Schütz (1979). Observations at selected transport distances from the Sahara showed no depletion of particles of diameter less then 4 μm until a 5000 km distance. The maximum of the volume distribution shifts from 100 μm in diameter to approximately 20, then 8 and finally 2 μm at 1000, 2000, and 5000 km, respectively. These observations were modeled assuming Stokes gravitational settling only, which however cannot explain the persistence of coarse particles larger than 10 μm observed after long-range transport. This puzzling point was raised again more recently by Maring et al. (2003). These authors compared measurements of the volume size distribution by a TSI Aerodynamic Particle Sizer (APS) on both sides of the Atlantic Ocean: on the Canary Islands and on Puerto Rico. They showed that the volume distributions are indistinguishable on both side of the Atlantic for particles smaller than 7.3 μm in diameter. To explain these observations, which are incompatible with assuming exclusively gravitational settling, they argued that the gravitational settling velocity could be counteracted by an additional and constant upward velocity. The physical processes that could bring about upward motion within the dust cloud are hypothesized (buoyancy by solar heating or turbulence) but not firmly identified. The calculations of Maring et al. (2003) also indicate that no significant change in the volume median diameter will occur after 2 days of transport. These conclusions were also reached by Reid et al. (2008) who analyzed APS measurements of volume distributions of dust from different origins at a receptor site in the United Arab Emirates.

Because of the strong dependence of the individual grain size on mineralogy, changes in the size distribution should affect the overall dust composition. From comparative sampling in the Sal Islands and on Barbados, Glaccum and Prospero (1980) found that the relative percent of clay-sized illite in the total dust mass increased during transport, whereas that of quartz decreased. A possible explanation for this change is the more rapid fallout of quartz, which has larger average diameter, and therefore higher settling velocity, than clay minerals. Other processes affecting the dust composition are referred as chemical aging. This mechanism occurs by cloud 'processing' or when a dust-laden air mass is entrained in the same transport region of polluted or oceanic air masses by horizontal and vertical winds. Two processes dominate, namely: (1) internal or external mixing between mineral dust and concurrent aerosol species derived from other sources (sea salt, fossil- and biomass-fuel combustion derived particles); and (2) heterogeneous reactions of secondary aerosol precursors (SO_2, H_2SO_4, NH_3, HNO_3) and combustion-driven pollutants (such as NOx, N_2O_5, NMHCs) on the surface of carbonate dust particles. Mixing and heterogeneous reactions are favored in those areas where mineral dust sources are located upwind from sea salt/biomass/anthropogenic pollution sources. The majority of studies concerning chemical aging of mineral dust occur in the outflow of Asian dust from Chinese deserts to the Japan Sea (Okada and Kai, 1995, 2004; Fan et al., 1996; Zhou et al., 1996; Clarke et al., 2004; Trochkine et al., 2003; Zhang et al., 2003a, b; Wang et al., 2005), but also in the eastern Mediterranean Sea (Falkovich et al., 2001; Sobanska et al., 2003). These studies are consistent in illustrating formation of not only secondary species such as sulfates and nitrates, but also some volatile organic carbon on the surface of aluminosilicates and carbonate particles. This effect results in accumulation of material on the surface of coarse particles having lower mass scattering efficiencies than the accumulation-mode particles that would have been formed in the absence of dust (Li-Jones et al., 1998; Clarke et al., 2004). In addition, an increase in the dust hygroscopicity induces greater cloud condensation and increased ice nuclei activity (DeMott et al., 2003; Perry et al., 2004).

The same effects are expected by particle mixing between scattering particles and dust. Observations also show that more than 60% of dust particles could become a mixture of dust and sea salt during the transport from China to Japan (Okada et al., 1990; Niimura et al., 1998; Zhang et al., 2003a). Sea salt and dust particles can be mixed internally (that is aggregated in the same particle) or externally (maintaining their identity as particles). The external mixing between light-absorbing carbon and dust particles, mostly in the size fraction of diameters lower than 0.6 μm, is documented (Clarke et al., 2004; Johnson et al., 2008; Kandler et al., 2007).

As a consequence of the size-selective mixing, the single scattering albedo of particles smaller than 0.6 μm in diameter is much lower (near 0.84 in the midvisible) than that of larger particles, where uncontaminated dust dominates (single scattering albedo on the order of 0.97). A lowered single scattering albedo would act toward enhanced atmospheric warming on bright continental surfaces such as deserts.

The scattering growth factor $f_{sca}(RH)$ as a function of the ambient relative humidity (RH), representing the enhancement in the particle scattering coefficient due to water uptake by mineral dust aerosol, has been measured to be between 1.1 and 1.7 (Li-Jones et al., 1998; Carrico et al., 2003; Howell et al., 2006; Kaaden et al., 2009), with lower values generally corresponding to dust measured close to the source region. Higher values correspond to mixtures. However, Carrico et al. (2003) showed that these higher values, which represent the humidity response of scattering, were dominated by the most hygroscopic of the components of the externally mixed aerosol, which is dominant over the internally mixed one, rather than to increased hygroscopicity of the dust particles due to internal mixing. Lack et al. (2009) also argued that dust/pollution mixing could be responsible for the enhanced absorption growth factor ($f_{abs}(RH)$ up to 1.5 at high RH) in dust plumes travelling over the Gulf of Mexico.

Information about dust particle shape from different regions has been recently gathered thanks to the development of computer-controlled electron microscopy (Reid et al., 2003a; Kandler et al., 2007; Coz et al., 2009). Particle shape is described by the aspect ratio (AR) defined as the ratio of the longest dimension to the orthogonal width of particles that are collected, by filtration or by impaction, on flat supports. Particles have the tendency of residing on whatever face has the largest surface area. As a consequence, the AR values from electron microscopy commonly reported in the literature are two-dimensional values that do not describe the volume-average particle morphology. Close to source regions, only a few studies report on the shape of dust particles in the third dimension (Okada et al., 2001; Chou et al., 2008).

The density distribution of two-dimensional AR values has been represented by a modified log-normal function as described by Kandler et al. (2007). Close to source regions in the Sahara, the AR density distribution ranges between 1 (spherical particles) and 5 (elongated particles). Median values are on the order of 1.6–1.7 (Chou et al., 2008; Kandler et al., 2007). The distribution of AR values shows only minor dependence on composition and on particle size.

Measurements offshore from the African coast indicate that the median aspect ratio does not change significantly during short-range transport (Kandler et al., 2007; Coz et al., 2009). Two different situations are reported concerning long-range transport. Measurements of air samples of long-range transported Saharan dust in Puerto Rico preserved the log-normal shape of the density distribution but showed a significantly higher median aspect ratio (1.9) (Reid et al., 2003c). This suggests a preferential removal of spherical particles. As a complement, the analysis of water-insoluble particles in Asian mineral dust deposited in snow layers on Mt. Tateyama in Japan showed significantly lower aspect ratios (median 1.22–1.31) and practically no values above 2.5 (Li and Osada, 2007). This would tend to suggest that spherical particles are removed preferentially from the atmosphere. The possibility that heterogeneous processing or the water uptake would change the single-particle shape distribution by leading to more soluble, lower aspect ratio particles, should be explored.

11.5.5 Impacts of Long-Range Transported Dust

11.5.5.1 Radiative Impact

Due to its large size range, mineral dust has the capability of interacting with both solar and terrestrial radiation. It is thus a crucial player in altering the radiative budget for regions over which it is transported. Depending on its composition (i.e., its complex refractive index), mineral dust may not only scatter but also absorb radiation. The scattering effect is dominant, particularly in the solar spectrum solar radiation, and leads to a decrease in incoming solar radiation at the surface. However, dust can also absorbs both solar and IR radiation, producing an atmospheric heating in the dust-laden atmospheric layers.

Field measurements of the radiative impact of mineral dust over transport regions are provided by several authors. These are best expressed in terms of direct radiative effect efficiency, corresponding to the flux perturbation normalized by the aerosol optical depth (DRE/AOD, units of $W\,m^{-2}$), therefore independent of the aerosol concentration. During the SHADE experiment (offshore Senegal for short-range transported dust), Haywood et al. (2003) reported solar-spectrum averaged upwelling radiative efficiency at the top of the atmosphere (TOA) of -87 to $-98\,W\,m^{-2}$ per unit of AOD measured at 0.55 μm. Christopher et al. (2003) reported on daily averaged TOA shortwave dust radiative force ranging from -7.1 to $-19\,W\,m^{-2}$ for AOD ranging from 0.17 to 0.33, respectively, during the PRIDE campaign over the Carribean.

Only few measurements exist of the radiative effect in the infrared spectrum. For the same episode investigated by Haywood et al. (2003), Highwood et al. (2003) reported a decrease in upwelling terrestrial radiation at the top of the atmosphere of $6.5\,W\,m^{-2}$ and an increase in downwelling terrestrial radiation at the surface of $11.5\,W\,m^{-2}$.

Based on multiple satellite data sets and a radiative model Zhu et al. (2007) estimated the shortwave (visible) and longwave (IR) radiative impact of dust downwind of eastern Asia, the Arabian Peninsula, and the Sahara Desert. The mean seasonal and regionally averaged reduction of radiative flux (visible + infrared) at the surface has been estimated in clear-sky conditions to about $5.9\,W\,m^{-2}$, $17.8\,W\,m^{-2}$, and $14.2\,W\,m^{-2}$, over the Yellow Sea, the Arabian Sea, and the west African coasts, respectively. The dust plume over the Arabian Sea was found to produce the largest effect on atmospheric heating mainly due to shortwave heating. The maximum longwave effect on heating rates occurs over the African coast downwind of the Sahara. It results in a strong cooling throughout the dust layer and moderate heating below. This large cooling inside the dust layer offsets up to 80% of the shortwave heating. Finally, the net radiative heating rate over the Yellow Sea is the smallest among these three regions.

This heating or cooling effect can impact atmospheric dynamics at both local and synoptic scales. In the eastern Atlantic, Wong et al. (2009) suggested that Saharan dust contributed to approximately 50% of the detected heating rate anomalies and thus has a substantial impact on atmospheric stability. This effect is also suspected to influence the development of cyclones and may explain a possible inhibition on the formation of tropical cyclones revealed by an anticorrelation between north tropical cyclone activity and Saharan dust cover (Evan et al., 2006). The additional heating induced by mineral dust can also lead to reduction in liquid water and cloud cover (Huang et al., 2006), causing the inhibition of cloud formation.

The impact of mineral dust on cloud formation, properties, and life time has not been investigated as intensively, with most of the studies on this indirect radiative impact being focused on finer and more soluble species. However, recent modeling studies highlight the possible contribution of mineral dust to the indirect radiative impact of aerosol though it has the ability to act as ice nuclei (Hoose et al., 2008).

11.5.5.2 Impact on Biogeochemistry

Atmospheric transport of dust particles can contribute significantly to the biogeochemical cycles of several elements and particularly nutrients. This is the case for iron and phosphorus that are considered as the main limiting factors in the growth of plants in marine ecosystems and on distant continents (Mahowald et al., 2007). As an example, deposition of Saharan dust contributes significantly to the budget of phosphorus in the Mediterranean basin (Bergametti et al., 1989). But this contribution can also be significant at much larger distances. This is the case in the Amazon for which Saharan dust contribute significantly to the annual phosphorus budget (Swap et al., 1992). Saharan dust was also suspected to play a role in the development of toxic red tides in Florida (Walsh et al., 2006). Saharan dust is a major contributor to soils in Florida, the Bahamas and Barbados (Muhs et al., 2007).

In some high-nutrient, low-chlorophyll remote oceanic areas, it was hypothesized that primary productivity (phytoplankton growth) was limited by the availability of iron (Martin, 1990). As a result, an increase in iron deposition can enhance biological activity and thus increase the capability of these ecosystems to act as a sink of CO_2. In many open-ocean regions the input of new iron to the surface waters is dominated by the atmospheric deposition of soluble iron in mineral aerosols (e.g., Fung et al., 2000; Sarthou et al., 2003). However, the aerosol iron fraction of importance in terms of the biogeochemical impact is the bioavailable fraction. As a proxy of this bioavailable fraction, soluble iron has been investigated in soils and aerosols.

Iron solubility appears to be higher in aerosols than in bulk soils ($\sim$0.5% of total iron; Hand et al., 2004). Journet et al. (2008) have shown that close to source regions, the variability in the iron solubility can be explained by differences in the aerosol mineralogical composition. Soluble iron is highest in clay minerals such as montmorrillonite and illite and lowest in iron oxides. Iron solubility in mineral dust can significantly increase during its transport due to chemical, photochemical and cloud processes (e.g., Jickells and Spokes, 2001; Desboeufs et al., 2001) and due to the size sorting induced by deposition processes that lead to an increase in clay contents in dust plumes (Baker and Jickells, 2006). Assessing the biogeochemical impact of mineral dust requires not only an estimation the dust deposition intensity but also information on its mineralogical composition and on the atmospheric processes to which dust is submitted during its long-range transport.

11.5.5.3 Dust as a Tracer of Climate

Although the most intense and active dust sources are located in the continental arid or semiarid regions located between 15° N – and 45° N, significant amounts of mineral dust occur in continental deposits, in oceanic sediments collected in remote oceanic regions (e.g., Grousset et al., 2003) and in polar ice caps (e.g., Biscaye et al., 1997). Mineral dust emissions and transport are extremely sensitive to meteorological and climatic conditions, so dust deposits provide long-term records that can help reconstructing past meteorology and climatology. Analysis of deep-sea sediments (Leinen and Sarnthein 1989; Hovan et al., 1991; Rea, 1994; deMenocal, 2004; Winckler et al., 2008; Martinez-Garcia et al., 2009) reveals large variations in dust accumulation rates in relation with glacial–interglacial cycles. Similar variations have also been identified in both Greenland and Antarctic ice cores (Thompson and Mosley-Thompson, 1981; Petit et al., 1999), with higher mineral dust fluxes associated with glacial periods. As an example, 30 times more dust was trapped in the Greenland ice cores during the last glacial maximum than today, but with large and abrupt variations in concentration (Grousset and Biscaye, 2005). Several proxies are used to interpret these paleorecords (Maher et al., 2010): Dust accumulation rate is used as a proxy of deposition fluxes, particle size changes have been widely used as an indicator wind strength in source regions or changes in the transport pathway, whereas mineralogy or isotopic signatures are used as fingerprints of dust origin. However, the variations of dust concentrations and properties occurring in paleorecords may reflect a variety of processes such as changes in the sources location that can be linked with changes in aridity conditions and vegetation cover or to the emergence of additional sources of glaciogenic silt and clay sediments derived from the continental shelves. Also important are changes in dust emission intensity due to modification of the circulation pattern and intensity from the local to the synoptic scale, changes in the transport efficiency and geographical pattern, and changes in deposition along the dust transport path (Maher et al., 2010). As a result, the interpretation of the changes in the dust deposition rates in past climates requires an ability to understand, describe, and quantify the present-day atmospheric pattern controlling dust emission, transport, deposition, and physical properties.

The analysis of present-day dust deposits in sediments and ice cores, in particular based on their isotopic signatures, has proven their usefulness in identifying differences in the sources of long-range transport and investigating their transport

pattern (Grousset and Biscaye, 2005). Rapid changes in dust origins due to seasonal variability in the transport path and efficiency can now be identified based on aerosol samples or thin layers of dust accumulation in undisturbed marine sediments or snow-pit layers. In the oceans, the combination of isotopic and mineralogical studies can help to distinguish and locate different sources, to reconstruct transport pathways, and finally to quantify the dust fluxes. Mineral dust is thus not only a paleotracer but also as a powerful tracer of present-day atmospheric circulation.

11.5.6 Conclusion

Our knowledge on long-transport of mineral dust has significantly increased in the past 10 years. In particular, the variability of dust transport in time and space, on horizontal and vertical scales, have been investigated thanks to the increasing capability of satellite observations, the instrumentation deployed during intensive field campaigns, and the availability and level of analysis of meteorological data. Although the atmospheric distribution of mineral dust is relatively well quantified, the total flux of dust involved in long-range transport is still uncertain, due to the fact that neither dust emission nor dust deposition are properly quantified. Prospero et al. (2010) highlighted the limitations of global dust models to reproduce the annual dust deposition and its seasonal pattern over Florida and interpret this limitation to be due to the range of variability of mineral dust life times in these models. Additional quantitative constraints on dust deposition rates and specific studies on the size-dependence of deposition processes, and the way they affect dust physical and chemical properties, are thus needed to make further progress in the quantification of mineral dust transport and its impacts. A large body of observations is indeed available concerning the composition and size distribution of long-range transported mineral dust, and data on the morphology of individual particles are recently also starting to be gathered. The analysis of the available data sets reveals a certain disparity in the sampling and analytical protocols, in particular in the instrumental passing efficiency affecting the reproduction of the particle size distribution, as well as the scarcity of coordinated observations along the transport pathways at different times after emission. Future systematic, process-oriented observations of particle composition, size, and morphology as a function of transport time are recommended.

Acknowledgments

We acknowledge the MODIS mission scientists and associated NASA personnel for the production of the data used in this research effort. The MODIS images from **Figure 1** are extracted from the MODIS images collection (http://visibleearth.nasa.gov/). Numerous analyses and visualizations used in this chapter (**Figures 3–5** and **9**) were produced with the Giovanni online data system, developed and maintained by the NASA GES DISC (Acker and Leptoukh, 2007) (http://disc.sci.gsfc.nasa.gov/giovanni/). The AERONET and PHOTONS staff and the PIs of the AERONET are warmly acknowledged for the contribution AERONET data provide for mineral dust studies. We thank Didier Tanré and Brent Holben and their staff for establishing and maintaining the sites of Dakar, Cape Verde and Barbados whose data are in this Figure 8 and related analysis. Bernadette Chatenet is also acknowledged for her active and long-term contribution to the maintaining of the site of Dakar and Cape Verde. The authors would like to thank Dan Muhs for his relevant comments and corrections and his careful reading of the manuscript. We also thank Christel Bouet for her help in producing **Figures 7** and **8**.

References

Acker, J.G., Leptoukh, G., 2007. Online analysis enhances use of NASA Earth science data. Eos, Transactions, AGU 88(2), 14–17.

Arimoto, R., Duce, R., Ray, B., Ellis, Jr. W., Cullen, J., Merrill, J., 1995. Trace elements in the atmosphere over the North Atlantic. Journal of Geophysical Research 100(D1), 1199–1213.

Baker, A.R., Jickells, T.D., 2006. Mineral particle size as a control on aerosol iron solubility. Geophysical Research Letters 33, L17608. http://dx.doi.org/10.1029/2006GL026557.

Bates, T.S., Quinn, P.K., Coffman, D.J., et al., 2004. Marine boundary layer dust and pollutant transport associated with the passage of a frontal system over eastern Asia. Journal of Geophysical Research 109, D19S19. http://dx.doi.org/10.1029/2003JD004094.

Bergametti, G., Dutot, A.-L., Buat-Menard, P., Losno, R., Remoudaki, E., 1989. Seasonal variability of the elemental composition of atmospheric aerosol particles over the northwestern Mediterranean. Tellus 41B, 353–361.

Biscaye, P.E., Grousset, F.E., Revel, M., et al., 1997. Asian provenance of glacial dust (stage 2) in the Greenland ice sheet project 2 ice core, summit, Greenland. Journal of Geophysical Research-Oceans 102(C12), 26765–26781.

Bory, A., Biscaye, P.E., Grousset, F.E., 2003. Two distinct seasonal Asian source regions for mineral dust deposited in Greenland (NorthGRIP). Geophysical Research Letters 30, 1167. http://dx.doi.org/10.1029/2002GL016446.

Cahill, C.F., 2003. Asian aerosol transport to Alaska during ACE-Asia. Journal of Geophysical Research 108(D23), 8664. http://dx.doi.org/10.1029/2002JD003271.

Cakmur, R.V., Miller, R.L., Tegen, I., 2001. A comparison of seasonal and interannual variability of soil dust aerosols over the Atlantic Ocean as inferred by the TOMS AI and AVHRR AOT retrievals. Journal of Geophysical Research 106(16), 18287–18303.

Caquineau, S., Gaudichet, A., Gomes, L., Legrand, M., 2002. Mineralogy of Saharan dust transported over northwestern tropical Atlantic Ocean in relation to source regions. Journal of Geophysical Research 107(D15), 4251. http://dx.doi.org/10.1029/2000JD000247.

Carlson, T.N., Prospero, J.M., 1972. The large-scale movement of Saharan air outbreaks over the northern equatorial Atlantic. Journal of Applied Meteorology 11(2), 283–297.

Carrico, C.M., et al., 2003. Mixtures of pollution, dust, sea salt, and volcanic aerosol during ACE-Asia: radiative properties as a function of relative humidity. Journal of Geophysical Research 108(D23), 8650. http://dx.doi.org/10.1029/2003JD003405.

Cheng, T., Lu, D., Wang, G., Xu, Y., 2005. Chemical characteristics of Asian dust aerosol from Hunshan Dake Sandland in Northern China. Atmospheric Environment 39, 2903–2911.

Chester, R., 1986. The marine mineral aerosol. In: Buat-Ménard, P. (Ed.), The Role of Air–Sea Exchange in Geochemical Cycling. D. Reidel Publishing Company, Dordrecht, pp. 443–476.

Chiapello, I., Bergametti, G., Chatenet, B., Bousquet, P., Dulac, F., Santos-Soares, E., 1997. Origins of African dust transported over the northeastern tropical Atlantic. Journal of Geophysical Research 102, 13701–13709.

Chiapello, I., Bergametti, G., Gomes, L., et al., 1995. An additional low layer transport of Sahelian and Saharan dust over the north-eastern tropical Atlantic. Geophysical Research Letters 22, 3191–3194.

Chiapello, I., Moulin, C., Prospero, J.M., 2005. Understanding the long-term variability of African dust transport across the Atlantic as recorded in both Barbados surface concentrations and large-scale Total Ozone Mapping Spectrometer (TOMS) optical thickness. Journal of Geophysical Research 110(D18), D18S10.

Chou, C., Formenti, P., Maille, M., et al., 2008. Size distribution, shape, and composition of mineral dust aerosols collected during the African monsoon multidisciplinary analysis special observation period 0: dust and biomass-burning experiment field campaign in Niger, January 2006. Journal of Geophysical Research 113, D00C10.

Chun, Y., 2000. Yellow sand phenomenon recorded in the Choson Dynasty Silok, Krean. Journal of Meteorological Society 36(2), 285–292.

Clarke, A.D., Shinozuka, Y., Kapustin, N., et al., 2004. Size distributions and mixtures of dust and black carbon aerosol in Asian outflow: physiochemistry and optical properties. Journal of Geophysical Research 109, D15S09. http://dx.doi.org/10.1029/2003JD004378.

Coz, E., Gómez-Moreno, F.J., Pujadas, M., Casuccio, G.S., Lersch, T.L. Artíñano, B., 2009. Individual particle characteristics of North African dust under different long-range transport scenarios. Atmospheric Environment 43, 1850–1863.

d'Almeida, G.A., Schütz, L., 1983. Number, mass and volume distributions of mineral aerosol and soils of the Sahara. Journal of Applied Meteorology 22(2), 233–243.

Darwin, C.R., 1846. An account of the fine dust which often falls on vessels in the Atlantic Ocean. Quarterly Journal of the Geological Society of London 2, 26–30.

Deepshikha, S., Satheesh, S.K., Srinivasan, J., 2006. Dust aerosols over India and adjacent continents retrieved using METEOSAT infrared radiance Part I: sources and regional distribution. Annales Geophysicae 24(1), 37–61.

Delany, A.C., Parkin, D.W., Griffin, J.J., Goldberg, E.D., Reimann, B.E.F., 1967. Airborne dust collected at Barbados. Geochimica et Cosmochimica Acta 31, 885–909.

deMenocal, P.B., 2004. African climate change and faunal evolution during the Pliocene-Pleistocene. Earth and Planetary Science Letters 220, 3–24.

DeMott, P.J., Sassen, K., Poellot, M.R., et al., 2003. African dust aerosols as atmospheric ice nuclei. Geophysical Research Letters 30(14), 1732. http://dx.doi.org/10.1029/2003GL017410.

Desboeufs, K.V., Losno, R., Colin, J.L., 2001. Factors influencing aerosol solubility during cloud processes. Atmospheric Environment 35, 3529–3537.

Duce, R.A., 1995. Sources, distributions, and fluxes of mineral aerosols and their relationship to climate. In: Charlson, R.J., Heintzenberg, J. (Eds.), Aerosol Forcing of Climate. Wiley, New York, pp. 43–72.

Duce, R.A., Unni, C.K., Ray, B.J., Prospero, J.M., Merrill, J.T., 1980. Long-range atmospheric transport of soil dust from Asia to the Tropical North Pacific-temporal variability. Science 209(4464), 1522–1524.

Evan, A.T., Heidinger, A.K., Knippertz, P., 2006. Analysis of winter dust activity off the coast of West Africa using a new 24-year over-water advanced very high resolution radiometer satellite dust climatology. Journal of Geophysical Research 111, D12210. http://dx.doi.org/10.1029/2005JD006336.

Falkovich, A.H., Ganor, E., Levin, Z., Formenti, P., Rudich, Y., 2001. Chemical and mineralogical analysis of individual mineral dust particles. Journal of Geophysical Research 106, 18029–18036.

Fan, X.-B., Okada, K., Niimura, N., et al., 1996. Mineral particles collected in China and Japan during the same Asian dust-storm event. Atmospheric Environment 30, 347–351.

Formenti, P., Andreae, M.O., Cafmeyer, J., et al., 2001. Saharan dust in Brazil and Suriname during the large-scale biosphere–atmosphere experiment in Amazonia (LBA) – Cooperative LBA Regional Experiment (CLAIRE) in March 1998. Journal of Geophysical Research 106, 14,919–14,934.

Formenti, P., Elbert, W., Maenhaut, W., Haywood, J., Andreae, M.O., 2003. Chemical composition of mineral dust aerosol during the Saharan Dust Experiment (SHADE) airborne campaign in the Cape Verde region, September 2000. Journal of Geophysical Research 108, 8576. http://dx.doi.org/10.1029/2002JD002648.

Fung, I.Y., Meyn, S.K., Tegen, I., Doney, S.C., John, J.G., Bishop, J.K.B., 2000. Iron supply and demand in the upper ocean. Global Biogeochemical Cycles 14(2), 697–700.

Garrett, T.J., Russell, L.M., Ramaswamy, V., Maria, S.F., Huebert, B.J., 2003. Microphysical and radiative evolution of aerosol plumes over the tropical North Atlantic Ocean. Journal of Geophysical Research 108(D1), 4022. http://dx.doi.org/10.1029/2002JD002228.

Gasso, S., Stein, A.F., 2007. Does dust from Patagonia reach the sub-Antarctic Atlantic Ocean? Geophysical Research Letters 34, L01801. http://dx.doi.org/10.1029/2006GL027693.

Glaccum, R.A., Prospero, J.M., 1980. Saharan aerosols over the tropical north Atlantic – mineralogy. Marine Geology 37, 295–321.

Grousset, F.E., Biscaye, P.E., 2005. Tracing dust sources and transport patterns using Sr, Nd and Pb isotopes. Chemical Geology 222(3–4), 149–167.

Grousset, F.E., Ginoux, P., Bory, A., Biscaye, P.E., 2003. Case study of a Chinese dust plume reaching the French Alps. Geophysical Research Letters 30(6), 1277. http://dx.doi.org/10.1029/GL016833.

Hand, J.L., Mahowald, N.M., Chen, Y., Siefert, R.L., Luo, C., Subramaniam, A., Fung, I., 2004. Estimates of atmospheric-processed soluble iron from observations and a global mineral aerosol model: biogeochemical implications. Journal of Geophysical Research 109, D17205. http://dx.doi.org/10.1029/2004jd00457.

Haywood, J.M., Francis, P., Osborne, S., et al., 2003. Radiative properties and direct radiative effect of Saharan dust measured by the C-130 aircraft during SHADE: 1. Solar spectrum. Journal of Geophysical Research 108. http://dx.doi.org/10.1029/2002JD002687.

Haywood, J.M., Pelon, J., Formenti, P., et al., 2008. Overview of the dust and biomass burning experiment and African monsoon multidisciplinary analysis special observing period-0. Journal of Geophysical Research 113, D00C17. http://dx.doi.org/10.1029/2008jD010077.

Heintzenberg, J., 2008. The SAMUM-1 experiment over Southern Morocco: overview and introduction. Tellus 61(1), 2–11 doi:10.111/j.1600-0889.2008.00403.x.

Herman, J.R., Bhartia, P.K., Torres, O., Hsu, C., Seftor, C., Celarier, E., 1997. Global distribution of UV-absorbing aerosols from Nimbus 7/TOMS data. Journal of Geophysical Research 102, 16,911–16,922.

Highwood, E.J., Haywood, J.M., Silverstone, M.D., Newman, S.M., Taylor, J.P., 2003. Radiative properties and direct effect of Saharan dust measured by the C-130 aircraft during Saharan Dust Experiment (SHADE): 2. Terrestrial spectrum. Journal of Geophysical Research 108, 8578. http://dx.doi.org/10.1029/2002jd002552.

Hoose, C., Lohmann, U., Erdin, R., Tegen, I., 2008. The global influence of dust mineralogical composition on heterogeneous ice nucleation in mixed-phase clouds. Environment Research Letters 3(025003), 14.

Hovan, S.A., Rea, D.K., Pisias, N., 1991. Late Pleistocene continental climate and oceanic variability recorded in northwest Pacific sediments. Paleoceanography 6(3), 349–370.

Howell, S.G., Clarke, A.D., Shinozuka, Y., et al., 2006. Influence of relative humidity upon pollution and dust during ACE-Asia: size distributions and implications for optical properties. Journal of Geophysical Research 111, D06205. http://dx.doi.org/10.1029/2004JD005759.

Huang, J., Lin, B., Minnis, P., et al., 2006. Satellite-based assessment of possible dust aerosols semi-direct effect on cloud water path over East Asia. Geophysical Research Letters 33, L19802. http://dx.doi.org/10.1029/2006GL026561.

Huang, J., Minnis, P., Chen, B., et al., 2008. Long-range transport and vertical structure of Asian dust from CALIPSO and surface measurements during PACDEX. Journal of Geophysical Research 113, D23212. http://dx.doi.org/10.1029/2008JD010620.

Huang, J., Minnis, P., Yi, Y., et al., 2007. Summer dust aerosols detected from CALIPSO over the Tibetan Plateau. Geophysical Research Letters 34, L18805. http://dx.doi.org/10.1029/2007GL029938.

Huang, J.F., Zhang, C.D., Prospero, J.M., 2010. African dust outbreaks: a satellite perspective of temporal and spatial variability over the tropical Atlantic Ocean. Journal of Geophysical Research 115, D05202.

Huebert, B.J., Bates, T., Russell, P.B., et al., 2003. An overview of ACE-Asia: strategies for quantifying the relationships between Asian aerosols and their climatic impacts. Journal of Geophysical Research 108(D23), 8633. http://dx.doi.org/10.1029/2003JD003550.

Husar, R., Prospero, J., Stowe, L., 1997. Characterization of tropospheric aerosols over the oceans with the NOAA advanced very high resolution radiometer optical thickness operational product. Journal of Geophysical Research 102(D14), 16889–16909.

Husar, R.B., Tratt, D.M., Schichtel, B.A., et al., 2001. Asian dust events of April 1998. Journal of Geophysical Research 106(D16), 18,317–18,330.

Jaenicke, R., Schütz, L., 1978. Comprehensive study of physical and chemical properties of the surface aerosols in the Cape Verde Islands region. Journal of Geophysical Research 83, 3585–3599.

Jickells, T.D., Spokes, L., 2001. Atmospheric iron inputs to the ocean. In: Turner, D., Hunter, K.A. (Eds.), Biogeochemistry of Iron in Seawater. Wiley, Hoboken, N.J., pp. 85–121.

Johnson, B.T., Osborne, S.R., Haywood, J.M., Harrison, M.A.J., 2008. Aircraft measurements of biomass burning aerosol over West Africa during DABEX. Journal of Geophysical Research 113, D00C06. http://dx.doi.org/10.1029/2007JD009451.

Journet, E., Desboeufs, K.V., Caquineau, S., Colin, J.-L., 2008. Mineralogy as a critical factor of dust iron solubility. Geophysical Research Letters 35, L07805. http://dx.doi.org/10.1029/2007GL031589.

Junge, C., 1979. The importance of mineral dust as an atmospheric constituent. In: Morales, C. (Ed.), Saharan Dust: Mobilization, Transport, Deposition. Wiley, New York, pp. 49–60.

Kaaden, N., Massling, A., Schladitz, A., et al., 2009. State of mixing, shape factor, number size distribution, and hygroscopic growth of the Saharan anthropogenic and mineral dust aerosol at Tinfou, Morocco. Tellus 61B, 51–63.

Kandler, K., Benker, N., Bundke, U., et al., 2007. Chemical composition and complex refractive index of Saharan mineral dust at Izana, Tenerife (Spain) derived by electron microscopy. Atmospheric Environment 41, 8058–8074.

Kobayashi, A., Hayashida, S., Okada, K., Iwasaka, Y., 1985. Measurements of the polarization properties of Kosa (Asian dust-storm) particles by a Laser Radar in Spring 1983. Journal of Meteorological Society Japan 63(1), 144–149.

Kubilay, N., Nickovic, S., Moulin, C., Dulac, F., 2000. An illustration of the transport and deposition of mineral dust onto the Mediterranean Sea. Atmospheric Environment 22, 1293–1303.

Kuloglu, E., Tuncel, G., 2005. Size distribution of trace elements and major ions in the eastern Mediterranean atmosphere. Water, Air, & Soil Pollution 167, 221–241.

Lack, D.A., Quinn, P.K., Massoli, P., et al., 2009. Relative humidity dependence of light absorption by mineral dust after long-range atmospheric transport from the Sahara. Geophysical Research Letters 36, L24805. http://dx.doi.org/10.1029/2009GL041002.

Laurent, B., Marticorena, B., Bergametti, G., Léon, J.F., Mahowald, N., M., 2008. Modeling mineral dust emissions from the Sahara desert using new surface properties and soil database. Journal of Geophysical Research 113, D14218. http://dx.doi.org/10.1029/2007JD009484.

Laurent, B., Marticorena, B., Bergametti, G., Mei, F., 2006. Modeling mineral dust emissions from Chinese and Mongolian deserts. Global and Planetary Change 52, 121–141.

Legrand, M., N'Doumé, C., Jankowiak, I., 1994. Satellite-derived climatology of the Saharan aerosol. In: Lynch, D.K. (Ed.), Passive Infrared Remote Sensing of Clouds and the Atmosphere II: Proceedings SPIE 2309, pp. 127–135.

Legrand, M., Plana-Fattori, A., N'Doumé, C., 2001. Satellite detection of dust using the IR imagery of Meteosat, 1, Infrared difference dust index. Journal of Geophysical Research 106(18), 251–274.

Leinen, M., Sarnthein, M., 1989. Paleoclimatology and Paleometeorology: Modern and Past Patterns of Global Atmospheric Transport. Kluwer Academic Publishers, Dordrecht, vol. 282, NATO ASI Series.

Léon, J.-F., Derimian, Y., Chiapello, I., et al., 2009. Aerosol vertical distribution and optical properties over M'Bour (16.96° W; 14.39° N), Senegal from 2006 to 2008. Atmospheric Chemistry and Physics 9(23), 9249–9261.

Levy, R.C., Remer, L.A., Mattoo, S., Vermote, E.F., Kaufman, Y.J., 2007. Second-generation operational algorithm: retrieval of aerosol properties over land from inversion of Moderate Resolution Imaging Spectroradiometer spectral reflectance. Journal of Geophysical Research 112(D13), D13211.

Li, J., Osada, K., 2007. Water-insoluble particles in spring snow at Mt. Tateyama, Japan: characteristics of the shape factors and size distribution in relation with their origin and transportation. Journal of the Meteorological Society of Japan 85, 137–149.

Li-Jones, X., Maring, H., Prospero, J., 1998. Effect of relative humidity on light scattering by mineral dust aerosol as measured in the marine boundary layer over the tropical Atlantic Ocean. Journal of Geophysical Research 103(D23), 31,113–31,121. http://dx.doi.org/10.1029/98JD01800.

Li-Jones, X., Prospero, J.M., 1998. Variations in the size distribution of non-sea-salt sulfate aerosol in the marine boundary layer at Barbados: impact of African dust. Journal of Geophysical Research 103, 16,073–16,084.

Liu, D., Wang, Z., Liu, Z., Winker, D., Trepte, C., 2008. A height resolved global view of dust aerosols from the first year CALIPSO lidar measurements. Journal of Geophysical Research 113, D16214. http://dx.doi.org/10.1029/2007JD009776.

Maenhaut, W., Ptasinski, J., Cafmeyer, J., 1999. Detailed mass size distributions of atmospheric aerosol species in the Negev desert, Israel, during ARACHNE-96. Nuclear Instruments and Methods in Physics Research B 150, 422–427.

Maher, B.A., Prospero, J.M., Mackie, D., Gaiero, D., Hesse, P.P., Balkanski, Y., 2010. Global connections between aeolian dust, climate and ocean biogeochemistry at the present day and at the last glacial maximum. Earth-Science Reviews 99, 61–97. http://dx.doi.org/10.1016/j.earscirev.2009.12.001.

Mahowald, N.M., Ballantine, J.A., Feddema, J., Ramankutty, N., 2007. Global trends in visibility: implications for dust sources. Atmospheric Chemistry and Physics 7, 3309–3339.

Marenco, F., Bonasoni, P., Calzolari, F., et al., 2006. Characterization of atmospheric aerosols at Monte Cimone, Italy, during summer 2004: source apportionment and transport mechanisms. Journal of Geophysical Research 111, D24202. http://dx.doi.org/10.1029/2006JD007145.

Maring, H., Savoie, D.L., Izaguirre, M.A., Custals, L., Reid, J.S., 2003. Mineral dust aerosol size distribution change during atmospheric transport. Journal of Geophysical Research 108(D19), 8592. http://dx.doi.org/10.1029/2002JD002536.

Marticorena, B., Bergametti, G., 1996. Two-years simulations of seasonal and interannual changes of the Saharan dust emissions. Geophysical Research Letters 23, 1921–1924.

Marticorena, B., Chatenet, B., Rajot, J.L., et al., 2010. Temporal variability of mineral dust concentrations over West Africa: analyses of a pluriannual monitoring from the AMMA Sahelian Dust Transect. Atmospheric Chemistry and Physics Discussion 10, 8051–8101.

Martin, J.H., 1990. Glacial-interglacial CO2 change: the iron hypothesis. Paleoceanography 5(1), 1–13.

Martinez-Garcia, A., Rosell-Melé, A., Geibert, W., et al., 2009. Links between iron supply, marine productivity, sea surface temperature, and CO_2 over the last 1.1 Ma. Paleoceanography 24, PA1207. http://dx.doi.org/10.1029/2008PA001657.

Merrill, J.T., Uematsu, M., Bleck, R., 1989. Meteorological analysis of long-range transport of mineral aerosols over the North Pacific. Journal of Geophysical Research 94, 8584–8598.

Middleton, N.J., 1986. A geography of dust storms in southwest Asia. Journal of Climatology 6, 183–196.

Mikami, M., Abe, O., Du, M., et al., 2002. The impact of Aeolian dust on climate: Sino-Japanese cooperative project ADEC. Journal of Arid Land Studies 11(4), 211–222.

Moulin, C., Chiapello, I., 2006. Impact of human-induced desertification on the intensification of Sahel dust emission and export over the last decades. Geophysical Research. Letters 33(18), L18808.

Moulin, C., Lambert, C.E., Dulac, F., Dayan, U., 1997. Control of atmospheric export of dust from North Africa by the North Atlantic Oscillation. Nature 387, 691–694.

Muhs, D.R., Budahn, J., Skipp, G., Prospero, J.M., Patterson, D., Bettis, E.A., 2010. Geochemical and mineralogical evidence for Sahara and Sahel dust additions to Quaternary soils on Lanzarote, eastern Canary Islands, Spain. Terra Nova 22(6), 399–410. http://dx.doi.org/10.1111/j.1365-3121.2010.00949.x.

Muhs, D.R., Budahn, J.R., Prospero, J.M., Carey, S.N., 2007. Geochemical evidence for African dust inputs to soils of western Atlantic islands: Barbados, the Bahamas, and Florida. Journal of Geophysical Research 112, F02009. http://dx.doi.org/10.1029/2005JF000445.

Niimura, N., Okada, K., Fan, X.-B., et al., 1998. Formation of Asian dust–storm particles mixed internally with sea salt in the atmosphere. Jounal of the Meteorological Society of Japan 76, 275–288.

Okada, K., Heintzenberg, J., Kai, K., Qin, Y., 2001. Shape of atmospheric mineral particles collected in three Chinese arid-regions. Geophysical Research Letters 28, 3123–3126.

Okada, K., Kai, K., 1995. Features and elemental composition of mineral particles collected in Zhangye, China. Journal of the Meteorological Society of Japan 73, 947–957.

Okada, K., Kai, K., 2004. Atmospheric mineral particles collected at Qira in the Taklamakan Desert, China. Atmospheric Environment 38, 6927–6935.

Okada, K., Naruse, H., Tanaka, T., et al., 1990. X-ray spectrometry of individual Asian dust–storm particles over the Japanese islands and the North Pacific Ocean. Atmospheric Environment 24A, 1369–1378.

Ott, S.T., Ott, A., Martin, D.W., Young, J.A., 1991. Analysis of a transatlantic Saharan dust outbreak based on satellite and GATE data. Monthly Weather Review 119(8), 1832–1850.

Perry, K.D., Cahill, T.A., Eldred, R.A., Dutcher, D.D., 1997. Long-range transport of North African dust to the eastern United States. Journal of Geophysical Research 102, 11225–11238.

Perry, K.D., Cliff, S.S., Jimenez-Cruz, M.P., 2004. Evidence for hygroscopic mineral dust particles from the intercontinental transport and chemical transformation experiment. Journal of Geophysical Research 109, D23S28. http://dx.doi.org/10.1029/2004JD004979.

Petit, J.R., Jouzel, J., Raynaud, D., et al., 1999. Climate and atmospheric history of the past 420,000 years from the Vostok ice core, Antarctica. Nature 399, 429–436.

Prospero, J.M., 1968. Atmospheric dust studies on Barbados. Bulletin of the American Meteorological Society 49, 645–652.

Prospero, J.M., 1999. Long-range transport of mineral dust in the global atmosphere: impact of African dust on the environment of the southeastern United States. Proceedings of the National academy of Sciences of the United States of America 96, 3396–3403.

Prospero, J.M., Carlson, T.N., 1981. Saharan air outbreaks over the tropical North Atlantic. Pageoph 119, 677–691.

Prospero, J.M., Ginoux, P., Torres, O., Nicholson, S.E., Gill, T.E., 2002. Environmental characterization of global sources of atmospheric soil dust identified with the Nimbus 7 Total Ozone Mapping Spectrometer (TOMS) absorbing aerosol product. Reviews of Geophysics 40(1), 1–31.

Prospero, J.M., Glaccum, R.A., Nees, R.T., 1981a. Atmospheric transport of soil dust from Africa to South America. Nature 289, 570–572.
Prospero, J.M., Glaccum, R.A., Nees, R.T., 1981b. Atmospheric transport of soil dust from Africa to South America. Nature 289, 570–572.
Prospero, J.M., Landing, W.M., Schulz, M., 2010. African dust deposition to Florida: temporal and spatial variability and comparison to models. Journal of Geophysical Research 115, D13304. D13304.http://dx.doi.org/10.1029/2009JD012773.
Prospero, J.M., Nees, R., 1977. Dust concentration in the atmosphere of the equatorial North Atlantic: possible relationship to the sahelian drought. Science 196, 1196–1198.
Prospero, J.M., Nees, R.T., 1986. Impact of the North African drought and El Niño on mineral dust in the Barbados trade wind. Nature 320, 735–738.
Prospero, J.M., Savoie, D.L., Carlson, T.N., Nees, R.T., 1979. Monitoring Saharan aerosol transport by means of atmospheric turbidity measurements. In: Morales, C. (Ed.), Saharan Dust: Mobilization, Transport, Deposition, SCOPE rep. 14. Wiley, New York, pp. 171–186.
Pye, K., 1987. Aeolian Dust and Dust Deposits. Academic Press, London, 334 pp.
Raes, F., Bates, T., McGovern, F., Van Liedekerke, M., 2000. The 2nd aerosol characterization experiment (ACE-2): general overview and main results. Tellus B. 52(2), 111–125.
Rea, D.K., 1994. The paleoclimatic record provided by aeolian deposition in the deep sea – the geologic history of wind. Review of Geophysics 32, 159–195.
Reid, E.A., Reid, J.S., Meier, M.M., et al., 2003a. Characterization of African dust transported to Puerto Rico by individual particle and size segregated bulk analysis. Journal of Geophysical Research 108(D19), 8591. http://dx.doi.org/10.1029/2002JD002935.
Reid, J.S., Jonsson, H.H., Maring, H.B., et al., 2003c. Comparison of size and morphological measurements of coarse mode dust particles from Africa. Journal of Geophysical Research 108(D19), 8593. http://dx.doi.org/10.1029/2002JD002485.
Reid, J.S., Kinney, J.E., Westphal, D.L., et al., 2003b. Analysis of measurements of Saharan dust by airborne and ground-based remote sensing methods during the Puerto Rico Dust Experiment (PRIDE). Journal of Geophysical Research 108(D19), 8586. http://dx.doi.org/10.1029/2002JD002493.
Reid, J.S., Stuart, J.P., Walker, A.L., et al., 2008. An overview of UAE2 flight operations: observations of summertime atmospheric thermodynamic and aerosol profiles of the southern Arabian Gulf. Journal of Geophysical Research 113, D14213. http://dx.doi.org/10.1029/2007JD009435.
Remer, L.A., Kaufman, Y.J., Tanré, D., et al., 2005. The MODIS aerosol algorithm, products, and validation. Journal of the Atmospheric Sciences 62(4), 947–973.
Sarthou, G., Baker, A.R., Blain, S., et al., 2003. Atmospheric iron deposition and sea-surface dissolved iron concentrations in the east Atlantic. Deep Sea Research, Part I 50, 1339–1352.
Schütz, L., 1979. Sahara dust transport over the North Atlantic Ocea – Model calculations and measurements. In: Morales, C. (Ed.), Saharan Dust. Wiley, New York, pp. 267–277.
Schutz, L., Sebert, M., 1987. Mineral aerosols and source identification. Journal of Aerosol Science 18(I), 1–10.
Smolik, J., Zdimal, V., Schwarz, J., et al., 2003. Size resolved mass concentration and elemental composition of atmospheric aerosols over the eastern Mediterranean area. Atmospheric Chemistry and Physics 3, 2207–2216.
Sobanska, S., Pauwels, B., Maenhaut, W., Adams, F., 2003. SEM-EDX Characterisation of Tropospheric Aerosols in the Negev desert (Niger). Journal of Atmospheric Chemistry 44, 299–322.
Sokolik, I.N., Toon, O.B., 1999. Incorporation of mineralogical composition into models of the radiative properties of mineral aerosol from UV to IR wavelengths. Journal of Geophysical Research 104(D8), 9423–9444. http://dx.doi.org/10.1029/1998JD200048.
Stowe, L.L., Ignatov, A.A., Singh, R.R., 1997. Development, validation and potential enhancement to the second generation operational aerosol product at NOAA/NESDIS. Journal of Geophysical Research 102, D14. http://dx.doi.org/10.1029/96JD02132.
Sun, J., Zhang, M., Liu, T., 2001. Spatial and temporal characteristics of dust storms in China and its surrounding regions, 1960–1999: relations to source area and climate. Journal of Geophysical Research 106, 10,325–10,333.
Swap, R., Garstang, M., Graco, S., Talbot, R., Kallberg, P., 1992. Sahara dust in the Amazon basin. Tellus 44B, 133–149.
Takayama, Y., Takashima, T., 1986. Aerosol optical thickness of yellow sand over the Yellow Sea derived from NOAA satellite data. Atmospheric Environment 20, 631–638.
Tanré, D., Haywood, J., Pelon, J., et al., 2003. Measurement and modeling of the Saharan dust radiative impact: overview of the Saharan dust experiment (SHADE). Journal of Geophysical Research 108(D18), 8574.
Taylor, S.R., McLennan, S.M., 1985. The Continental Crust: Its Composition and Evolution. Blackwell, Cambridge, Mass.
Thompson, L.G., Mosley-Thompson, E., 1981. Microparticle concentration variations linked with climatic change: evidence from polar ice cores. Science 212, 812–815.
Torres, O., Bhartia, P.K., Herman, J.R., Ahmad, Z., Gleason, J., 1998. Derivation of aerosol properties from satellite measurements of backscattered ultraviolet radiation: theoretical basis. Journal of Geophysical Research 103, 17,099–17,110.
Trochkine, D., Iwasaka, Y., Matsuki, A., et al., 2003. Mineral aerosol particles collected in Dunhuang, China, and their comparison with chemically modified particles collected over Japan. Journal of Geophysical Research 108, 8642. http://dx.doi.org/10.1029/2002JD003268.
Tsunogai, S., Kondo, T., 1982. Sporadic transport and deposition of continental aerosols to the Pacific Ocean. Journal of Geophysical Research 87(C11), 8870–8874.
Uematsu, M., Duce, R.A., Prospero, J.M., Chen, L., Merrill, J.T., McDonald, R.L., 1983. Transport of mineral aerosol from Asia over the North Pacific Ocean. Journal of Geophysical Research 88, 5343–5552.
Uematsu, M., Merrill, J.T., Duce, R.A., Propero, J.M., 1986. Atmospheric fluxes of Asian desert dust to the North Pacific: temporal and spatial variability. Atmospheric Environment 20(10), 2073.
Uno, I., Eguchi, K., Yumimoto, K., et al., 2009. Asian dust transported one full circuit around the globe. Nature Geosciences 2, 557–560. http://dx.doi.org/10.1038/NGE0583.
Walsh, J.J., Jolliff, J.K., Darrow, B.P., et al., 2006. Red tides in the Gulf of Mexico: where, when, and why? Journal of Geophysical Research 111, C11003. C11003.http://dx.doi.org/10.1029/2004JC002813.
Wang, Y.Q., Zhang, X.Y., Arimoto, R., Cao, J.J., Shen, Z.X., 2005. Characteristics of carbonate content and carbon and oxygen isotopic composition of northern China soil and dust aerosol and its application to tracing dust sources. Atmospheric Environment 39(14), 2631–2642.
Wendisch, M., Coe, H., Baumgardner, D., et al., 2004. Aircraft particle inlets: state-of-the-art and future needs. Bulletin of the American Meteorological Society 85, 89–91. http://dx.doi.org/10.1175/BAMS-85-1-89.
Winckler, G., Anderson, R.F., Fleisher, M.Q., McGee, D., Mahowald, N., 2008. Covariant glacial–interglacial dust fluxes in the equatorial Pacific and Antarctica. Science 320, 94. http://dx.doi.org/10.1126/science.1150595.
Wong, S., Dessler, A.E., Mahowald, N.M., Yang, P., Feng, Q., 2009. Maintenance of lower tropospheric temperature inversion in the Saharan Air Layer by dust and dry anomaly. Journal of Climate 22(19), 5149–5162. http://dx.doi.org/10.1175/2009JCLI2847.1.
Zhang, D., Iwasaka, Y., Shi, G., Zang, J., Matsuki, A., Trochkine, D., 2003a. Mixture state and size of Asian dust particles collected at southwestern Japan in spring 2000. Journal of Geophysical Research 108, 4760. http://dx.doi.org/10.1029/2003JD003869.
Zhang, D., Zang, J., Iwasaka, Y., Shi, G., Matsuki, A., Trochkine, D., 2003b. Mixture state of Asian dust particles at a coastal site of Qingdao, China. Atmospheric Environment 37, 3895–3901.
Zhang, R., Arimoto, R., An, J., Yabuki, S., Sun, J., 2005. Ground observations of a strong dust storm in Beijing in 2002. Journal of Geophysical Research 110, D18S06. http://dx.doi.org/10.1029/2004JD004589.
Zhou, M., Okada, K., Qian, F., et al., 1996. Characteristics of dust storm particles and their long-range transport from China to Japan – case studies in April 1993. Atmospheric Research 40, 19–31.
Zhu, A., Ramanathan, V., Li, F., Kim, D., 2007. Dust plumes over the Pacific, Indian, and Atlantic oceans: climatology and radiative impact. Journal of Geophysical Research 112, D16208. http://dx.doi.org/10.1029/2007JD008427.

Biographical Sketch

Béatrice Marticorena is a scientist at French Centre National de Recherche Scientifique (CNRS). Her research field is the modeling of mineral dust emissions and mineral dust cycle. She has developed a physically explicit dust emission scheme and methodologies to map the relevant surface parameters over the Sahara desert and the deserts of eastern Asia. She participates in the development and validation of a regional model of the mineral dust cycle. She was involved in the coordination of the activities related to tropospheric aerosols within the framework of the AMMA (African Monsoon Multidisciplinary Analysis) international program. Since 2006, she is the PI of network composed of three ground stations dedicated to mineral dust monitoring in the Sahel.

Paola Formenti is a scientist at French Centre National de Recherche Scientifique (CNRS). Her research field is the *in situ* measurement of the physico-chemical and optical properties of mineral dust relevant to their effect on the radiative budget in the atmosphere. As an experimentalist, she has developed dedicated instrumentation, ground-based and airborne, to sample the relevant size-dependent aerosol properties. She is now the PI of the PEGASUS (Portable Gas and Aerosol Sampling Unit) mobile station, which is now being developed as a research and monitoring observational tool. She was involved in the coordination of the activities related to tropospheric aerosols within the framework of the AMMA (African Monsoon Multidisciplinary Analysis) international program, and in the incoming FENNEC and Charmex projects.